Transportation Research Part D 150 (2026) 105064

Contents lists available at ScienceDirect

Transportation Research Part D

journal homepage: www.elsevier.com/locate/trd

# Development of realistic driving cycles via incremental Markov chains for sport motorcycles

Adelmo Niccolai *, Lorenzo Berzi , Niccolò Baldanzini

*Universita degli Studi di Firenze Dipartimento di Ingegneria Industriale, Italy*

ARTICLE INFO

*Keywords:*
Synthetic driving cycle
Sport motorcycle
Markov chain
Real-word data; fuel consumption

ABSTRACT

Driving cycles are essential for vehicle certification, fuel consumption and emissions estimation. However, current approval cycles do not accurately capture the dynamics of sport motorcycles, leading to misrepresentation of riding conditions. This study addresses this gap by developing the Sport Motorcycle Driving Cycle (SMDC) using real-world data collected from a high-performance motorcycle. Data analysis revealed that key indicators, as the characteristic acceleration ($\tilde{a}$) and aerodynamic speed ($V^2_{\mathrm{aer}}$), differ significantly from type-approval cycles and strongly correlate with fuel consumption and engine power. The SMDC was synthesized via a novel method combining a 3D Markov Chain (speed, acceleration, and road slope) with incremental random walks. This approach achieved an energy consumption error of -0.31 % while reducing the cycle length by 90.7 % compared to the reference dataset. These results underscore the discrepancies between approval cycles and real sport riding, advocating for revised homologation protocols and offering a new tool for design and evaluation.

## 1. Introduction

Driving cycles (DCs), or speed profiles, are sequences of longitudinal speed values over time. The DCs were created since the early 70s to summarize the vehicle's typical operating conditions and are used in many fields, such as for testing pollution/exhaust emission, vehicle design, engine tuning, and riding range estimation. The DCs should reflect real-world driving conditions and be long enough to represent the driving data well, but not too much to be inefficient during the dynamometer or engine test.

The International Energy Agency (IPCC, 2022) indicates that transportation accounts for 23 % of worldwide greenhouse gas emissions. In a joint mission to mitigate the environmental footprint of mobility, scientists and industry experts have developed alternatives to accelerate the transition to sustainable transportation. The discrepancy between real-world driving and standard cycles suggested using dedicated real-world DC for studying vehicle consumption (Lien et al., 2024; Dornoff et al., 2020) and to prepare for the so-called Real Driving Emission (RDE) testing. Moreover, the European Association of Motorcycle Manufacturers (ACEM) acknowledges the EU's objective to achieve net-zero carbon emissions by 2050 (ACEM - European Association of Motorcycle Manufacturers, 2021). Battery electric vehicles (BEVs) have the potential to play a key role in transport decarbonization.

Motorcycles can be segmented by emphasizing features and targets, such as the rider posture, handling, etc. Sport motorcycles are designed for both roads and racing, featuring an aerodynamic rider seat that allows lateral movement during cornering. In the case of internal combustion engine sport motorcycles, medium to larger engine displacements (600-1000 cc) are also referred to as supersport

* Corresponding author.
*E-mail addresses:* adelmo.niccolai@unifi.it, adeniccolai@gmail.com (A. Niccolai), lorenoz.berzi@unifi.it (L. Berzi), niccolo.baldanzini@unifi.it (N. Baldanzini).

https://doi.org/10.1016/j.trd.2025.105064
Received 19 December 2024; Received in revised form 23 September 2025; Accepted 13 October 2025
Available online 15 November 2025

and hypersport, respectively (Lot, 2021). Among the driving cycles developed, there is no description of a sport motorcycle ride. As shown in Section 2.4, the international type approval cycle is not fully able to represent high-performance motorcycle riding. The Sport Motorcycle Driving Cycle (SMDC) was developed from real-world data, including road slope, by introducing the incremental 3D Markov Chain Monte Carlo construction method.

Sport motorcycles represent 13.6 % of the global market, which is worth USD 115,720 Mn in 2018 (Cadavid and Salazar-Serna, 2021). Smaller motorcycles outperform larger ones in terms of eco-friendliness, largely due to the distinct driving habits of larger bikes, and urban commuting generally results in a significantly lower environmental footprint per kilometer compared to highway travel (Cox and Mutel, 2018). A comparison of emissions depending on several motorcycle driving cycles found that CO emissions increased with engine size (Kumar et al., 2011). From this point of view, larger motorcycles such as sport motorcycles will benefit from a shift toward electrification; from another point of view, the electric traction characteristics fitted into a sport motorcycle could also appeal to high-demanding customers, improving riding experience per se. E-bikes and mid-size electric two-wheelers are the most energy-efficient powered vehicles for personal road transport. Replacing conventional two-wheelers with electric ones can reduce tank-to-wheel energy use by 50–90 %, primarily due to the higher efficiency of electric machines (Weiss et al., 2015). Although the possibility that two-wheelers can be used for urban transportation and personal commuting is more sustainable than passenger cars, only e-bikes have immediate market potential due to the added value provided by the power assistance. High cost and low perceived value of added characteristics, however, still prevent the adoption of mid-size and large electric two-wheelers. Examining the business model, the total cost of ownership (TCO) for electric motorcycles (EMs) is primarily attributed to the powertrain. For example, in Vietnam, the EMs have a TCO more than twice that of ICE motorcycles (Tran et al., 2023), in China, EMs already have a lower TCO, while in India, TCO is lower due to the incentives (IEA, 2024). Despite favourable TCO, the high initial cost represents a significant barrier to adoption (Truong et al., 2024). Consumer attitudes help predict the adoption of EM, and perception of instrumental attributes, such as range and speed, is related to the adoption of electric motorcycles (Eccarius and and, 2020; Yuniaristanto et al., 2022). According to these elements, improving powertrain design by applying so-called rightsizing criteria is crucial for reducing the cost and achieving optimal performance. This process begins with a well-representative driving cycle tailored to the specific purpose. Furthermore, the availability and accessibility of public and private charging stations are key determinants of purchase intention (Yuniaristanto et al., 2022), shaping not only the riding phase but also the trip-chaining experience. In this context, the proposal of a new driving cycle is aimed at better describing the category of high-performance motorcycles, with the results, even if based on internal combustion vehicles, serving as enablers for the proper design of electric motorcycles.

### 1.1. Driving cycles overview

The duration of the driving cycle is an essential element in assessing its effectiveness and its representativeness in typical case studies. A too short driving cycle might not accurately capture fuel consumption (Cui et al., 2021, 2022). Typically, standard driving cycles have lengths ranging from 600 to 2400 s (Giakoumis, 2017; Cui et al., 2021). Type approval driving cycles (e.g., NEDC, WLTP) may fail to accurately represent local driving patterns due to variations in infrastructure, traffic conditions, geography, and vehicle types (Hull et al., 2024; Grano et al., 2025). For these latter reasons, many DCs were developed, varying the type of vehicle and the driving conditions to capture unique region-specific driving behaviors. Good examples are the motorcycle speed schedules created for specific cities due to the lack of representation of current DCs (Tong et al., 2011; Saleh et al., 2009). The speed profiles can be divided into two categories: simple-modal and true transient. The former speed profiles are constructed by combining driving modes such as constant speed, constant acceleration, and idling. The J10 and the ECE15 are examples of modal driving cycles and simplify the real driving condition, while the true transient profiles maintain real-world data and values such as the World Motorcycle Test Cycles (WMTC). Among these two driving cycle types, the transient cycles are currently adopted due to better vehicle driving representation. The topic is widely described in the literature and continuously updated. Summary of motorcycle real-world driving cycles, data acquisition, exhaust emissions analysis, and cycle construction method can be found in the literature (Sithananthan and Kumar, 2021; Kusalaphirom et al., 2022). Table 1 reports relevant transient cycles with year, data collection method, construction method, geographic area, and engine displacement.

Engine displacement of the test vehicles varies from 50 cc motorcycles up to 1500 cc motorcycles, and electric scooters with a 3.7 kWh battery capacity and 3.3 kW of power. Geographically, the research spans locations including Taipei, Taichung, Kaohsiung, and Pingtung County in Taiwan, Edinburgh in the UK, Hanoi in Vietnam, Dhanbad and Vellore in India, Khon Kaen in Thailand, and Isfahan in Iran. The WMTC also collected data from Europe, Japan, China, and the USA. The developed motorcycle DCs are primarily based on commuting and urban riding of small motorcycles, and the road slope is not considered. These conditions may be different from sport motorcycle riding. The quantity of data collected varies widely: the total driving data can range from 44 trips (Saleh et al., 2009) to 442 cycles (total of 109 hours) (Tzeng and Chen, 1998), and from 70000 speed-time data points (Ghaffarpasand et al., 2021) to 210000 s (Gurusamy and Ashok, 2024). The WMTC, by comparison, is based on 518 hours of driving, covering a total distance of 27,224 km.

Cycle construction methods primarily rely on statistical similarity measures to identify or synthesize a representative cycle from real-world data. Common approaches include selecting the cycle or run with the “least total variance” (Chen et al., 2003), the “smallest Euclidean distance” (Chen et al., 2003), or the “minimum sum of absolute relative errors” (Tsai et al., 2005; Saleh et al., 2009). Many studies in Table 1 employ a “random selection approach” where micro-trips (short segments of driving) are randomly combined to form the cycle, to match overall statistical characteristics.

Driving cycles were designed for a diverse range of vehicles, primarily emphasizing passenger cars, spanning petrol, diesel, electric, and hybrid models (Bishop and Axon, 2024; Kamel and Huzayyin, 2024). A summary of typical case studies is provided here. A DC

**Table 1**
Collection of transient motorcycle driving cycles.

| Driving cycles | Country | Data collection | Engine displacement | Construction method |
|---|---|---|---|---|
| FTP 75 (Kruse and Huls, 1973) | USA | onboard measurement | unknown | micro-trip |
| TMDC (Tzeng and Chen, 1998) | Taipei | chasing technique | 50, 90, 125 cc | run with least total variance |
| 5 Asian city (Chen et al., 2003) | Asia | chasing technique | 150 cc (chaser motorcycle) | run with least total variance |
| WMTC (UNECE, 2014) | Worldwide | onboard measurement | 50–1500 cc | micro-trip |
| KHM (Tsai et al., 2005) | Taiwan | chasing technique | 125 cc (chaser motorcycle) | micro-trip |
| EDMC (Saleh et al., 2009) | Scotland | onboard measurement | 550 - 1000 cc | run with least relative error |
| CEMDC (Tong et al., 2011) | Vietnam | onboard measurement | 100 cc | micro-trip |
| KMDC (Seedam et al., 2015) | Thailand | chasing technique | 113 cc (chaser motorcycle) | micro-trip |
| Dhanbad DC (Adak et al., 2016) | India | onboard measurement | < 200 cc | micro-trip |
| KKMDC (Koossalapeerom et al., 2019) | Thailand | onboard measurement | 1000 W, 108 cc | micro-trip |
| IMDC (Ghaffarpasand et al., 2021) | Iran | onboard measurement | 125, 150, 200 cc | micro-trip |
| Real world eco-drive(Kusalaphirom et al., 2022) | Thailand | onboard measurement | 113 cc | micro-trip |
| E2WDC (Gurusamy and Ashok, 2024) | India | chasing technique and onboard measurement | 3.3 kW | Hybrid approach based on micro-trip |

based on different passenger cars and data collected from 2011 to 2018 was developed via the Markov chain method in London (Bishop and Axon, 2024). In Korea, a DC was generated for electric cars for urban, rural, and motorway use through a micro-trip analysis, K-means clustering, and Markov Chain, using the speed acceleration probability distribution (SAPD) as an assessment for valid cycles (Lee et al., 2025). A large dataset of 43 light-duty vehicles was used to develop a DC in Greater Cairo, showing that the Markov chain method outperformed the micro-trip method (Kamel and Huzayyin, 2024). For buses, different DCs were developed, like for paratransit (9–16 passengers) in Stellenbosch (Hull et al., 2024), electric bus in Hong Kong (Tong, 2019), electric bus including road grade change (Tong and Ng, 2023), and urban bus in Spain calculating the elevation via digital models. Finally, heavy-duty vehicle DCs were developed in Karnataka via 42-ton and 48-ton trucks using 0.4-0.5 million speed records (Gavimath and Ravuri, 2025).

Even though many DCs for motorcycles were developed, they were mainly based on low-power vehicles and commuting trips in high-density populated urban areas. Traffic and road topology are fundamental characteristics that influence driving style (Bishop and Axon, 2024). Designing high-performance motorcycles, the performance needed in typical riding might differ from the type approval cycles. Indeed, a difference in driving was found among vehicle performance levels, with the tendency of having higher speed and steeper acceleration in high-powered cars (power-to-mass > 61 W/kg) (André et al., 2006), suggesting that a more appropriate cycle should be used. Several metrics were developed to describe and compare DCs to each other, such as the duration, average speed, distance traveled, etc. A review of driving cycle metrics, often referred to as Characteristic Parameters (CPs), grouped by five categories related to physical dimension (time, speed, acceleration, stop, and dynamics), can be found in (Berzi et al., 2016), which can be used for a quantitative description. Another important tool is the speed acceleration probability distribution (SAPD), which describes the driving data probability to be of a certain speed and acceleration class (Hung et al., 2007). Different studies for developing motorcycles used many parameters like 10 (Ghaffarpasand et al., 2021), 11 (Tsai et al., 2005), and 12 (Tzeng and Chen, 1998; Saleh et al., 2009; Tong et al., 2011). The works on passenger cars and buses found 3 (Quirama et al., 2021), 13 (Tong, 2019; Tong and Ng, 2023), 16 (Lee and Filipi, 2011), and 26 (Bishop and Axon, 2024) as main parameters.

An appropriate DC is necessary for the right vehicle design and might provide valuable information to correctly size the powertrain components. Considering the outstanding performances of which sport motorcycles are typically capable (e.g., max speed over 200 km/h, power to mass ratio > 0.5 kW/kg), the use of the current cycles might fail to provide an accurate estimation of energy consumption and powertrain effort in case of specific applications (e.g., track riding), thus failing in assessing the range available for the user and the correct environmental impact. Furthermore, the legislative DCs do not consider the road slope influence. As expected, the road slope significantly affects emissions (Jia et al., 2021; Salihu et al., 2023) and should be included in the development of the driving cycle, especially for heavier vehicles (Jia et al., 2021). Various methodologies have been developed to address this gap. Some researchers have employed Markov chain methods to capture real-world behavior and include road grade, such as for electric scooters (Bishop et al., 2012), or for heavy-duty vehicles, by combining a 2D Markov chain with an average speed-based matching algorithm to simplify the complex 3D Markov model (Jia et al., 2021). The Markov Chain Monte Carlo (MCMC) process has also been utilized to develop urban driving cycles with road slope profiles, considering road type weights and digital surface models (DSM) (Bhatti et al., 2021). Furthermore, the micro-trip approach, often refined to include gradient, has been adapted in military areas to derive gradient-sensitive cycles based on fuel consumption criteria (Han et al., 2012), or by using clustering algorithms like k-means to group micro-trips into specific road grade classes (Salihu et al., 2023), revealing how acceleration and deceleration patterns vary with slope. This approach has also been used to develop electric bus driving cycles in hilly environments by classifying micro-trips into positive, negative, and zero gradient bins (Tong and Ng, 2023). Although the micro-trip cycle construction method was applied via novel modifications to create consistent slope and speed profiles over time, a margin of error in altitude changes must be applied (Maharaj and King, 2023). Research suggests that for maintaining their interdependence, the road-slope profile and speed should be concurrently synthesized (Silvas et al., 2016). Another study analyzes different Markov Chain models, indicating that 3D models (speed, acceleration, road slope) are mostly appropriate for the assessment of driving energy consumption (Topić et al., 2020). This study shows that the road slope affects the fuel consumption in terrains with significant elevation changes, and then the road slope was implemented in DC synthesis via a 3D Markov chain model.

The procedure to construct a driving cycle can be summarised in five main steps: route and vehicle selection, data collection, data analysis, using a construction method to develop driving cycles, and validation. The choice of the route and vehicle defines the set of driving data and should be chosen carefully. After selecting the route, the driving data can be collected with two methods: the chase technique or the instrumented ego vehicle. The chase method is based on chasing other vehicles with an instrumented vehicle and trying to perform the same behavior as the "prey" vehicle. Using an instrumented ego vehicle directly collects the driving data, and it is easier to register more than just the speed values. After gathering data, they are analyzed to extract the features or metric parameters, find patterns, and cluster to describe the typical driving condition (André, 2004). Through a cycle construction method, data are converted into one or more driving cycles, which summarize the characteristic dataset. As the last step, all the constructed cycles are compared with the reference data via a set of characteristic parameters (CPs), called Performance Value (PV) (Tong et al., 1999; Lin and Niemeier, 2003). The cycle with the lowest performance value is usually chosen among the others; thus, the PV definition is crucial for the final result. Different threshold deviations were applied; in general, values between 5 and 10 % were used.

### *1.2. Cycle construction methods*

The cycle construction method is fundamental for building a representative driving cycle that mimics real-world data. Different construction methods have been developed, which can be collected into four main classes: micro-trip cycle, segment-based, pattern classification, and stochastic modal cycle (Dai et al., 2008; Giakoumis, 2017). A brief description of all these methods will be provided, and more details can be found in previous works (Dai et al., 2008; Xiao et al., 2012; Giakoumis, 2017).

The first method is based on micro-trips (MT), which are the driving activities between two stops, and it was the most common building method. The micro-trips are extracted from the data and chained together to build a longer trip. MTs can be added via random selection, quasi-random selection, or searching for specific characteristics. The micro-trip itself does not differentiate between modal events like cruising and acceleration, or consider the temporal interdependence of modal activities (Lin and Niemeier, 2002). Different approaches were implemented to expand this method, such as classifying the micro-trip in speed bins. Several driving cycles were constructed using this method as reported in Table 1.

The segment-based approach is similar to the micro-trips, with the difference that segmentation is based on changes in roadway type in addition to stopping (Carlson and Austin, 1997). The segments are then chained with random or best-incremental logic until the desired length is reached. The segments in this method can start at any speed value; thus, particular attention is needed to connect them. The major applications of this construction method were the U.S. EPA facility-specific speed correction cycles, and the Australian CUEDC (Carlson and Austin, 1997; Brown et al., 1999).

The pattern classification divides the speed into "kinematic sequences" and classifies them into heterogeneous classes (André et al., 1995). The segments are then added randomly with the probability and time series of the kinematic sequences. This type of construction method was applied for constructing the European driving cycles under the ARTEMIS project (André et al., 1995; André, 1996, 2004).

Finally, the stochastic modal approach is based on predicting a sequence of driving activities by some stochastic model, like the Markov Chain and Monte Carlo (MCMC). This latter method can model the driving behavior and be used to build driving cycles based on features extracted from real-world data (Shi et al., 2016). The choice of the features is essential for a correct representation, like the longitudinal speed and velocity that can be used successfully to synthesize speed profiles (Lee and Filipi, 2011). The speed and acceleration were used in many other works, but more features can be selected, like the yaw rate (Esser et al., 2018), road slope (Silvas et al., 2016), or added a posteriori (Jia et al., 2021). There are no limits to the number of features, and a general multidimensional approach has already been applied, adding a lateral dynamics parameter as well (Esser et al., 2018). A comparison between the Markov chain and micro-trips method for light-duty vehicles highlighted the better outperforms of the former method and showed the poor representation of the reference and approval cycles (WLTP, NEDC, UDDS, and FTP-17) (Kamel and Huzayyin, 2024). Furthermore, the Transition Probability Matrix (TPM) can store a large amount of data without expanding its dimensions. Indeed, defining a finite number of states and adding more data will change the transition probability values, without increasing

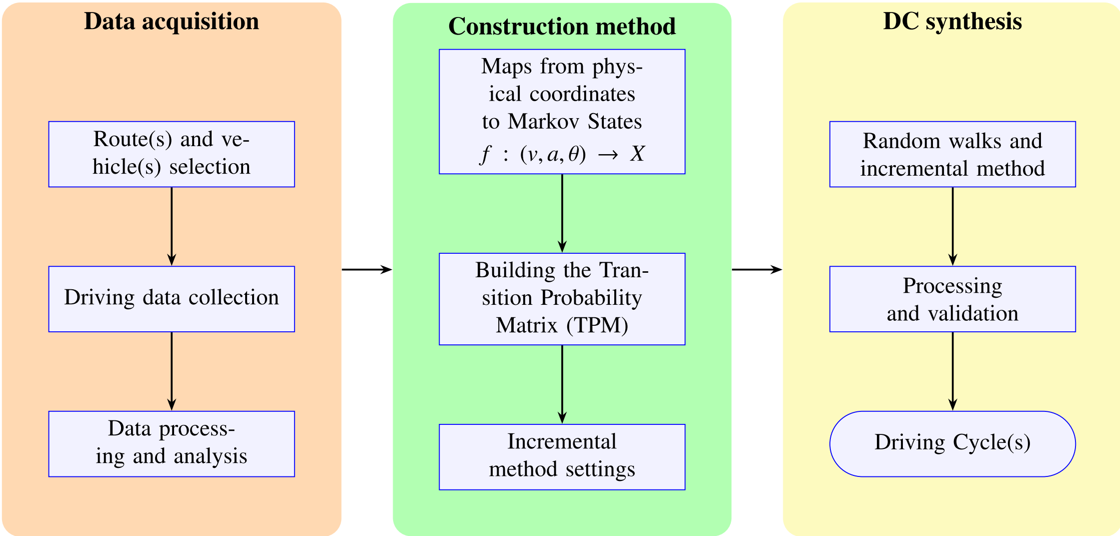


**Fig. 1.** Shows the procedure to synthesize a driving cycle from real-world driving data.

the matrix dimension or needing to store all the vehicle runs. In addition, the TPM collects information of the SAPD and speed-time sequence, building a link between them (Shi et al., 2016).

A Combination of two or more approaches was pursued, like the micro-trip and Markov chain method. The hybrid MT-MC method, for example, was applied to synthesize a driving cycle in Beijing, with micro-trips clustered by bin speed and assigned to a nine-by-nine transition probability matrix (Wang et al., 2019). Another study, based on a large number of vehicles (459 passenger cars), divided the trip profiles into micro-trips and then defined driving modes (clustering), linking them to a seven-by-seven transition probability matrix (Ma et al., 2019). Many other studies have applied hybrid techniques for developing driving cycles (Wang et al., 2020; Peng et al., 2020; Qiu et al., 2022; Yang et al., 2023; Ye et al., 2023; Kamel and Huzayyin, 2024), which are based on data collection, principal component analysis, data clustering, and the use of stochastic or genetic algorithms to generate a speed profile.

Among all these methods, a new construction method was proposed here, based on the well-known Markov Chain and Monte Carlo method, adding incremental random walks, with benefits in terms of driving cycle efficiency. This method autonomously defines the DC length from defining the duration, once the error in the performance values is set.

In conclusion, this work aims to develop a specific driving cycle for future electric sport motorcycles that accounts for road slope, addressing the current lack of representative driving cycles for sport motorcycles in the literature. The study offers three main contributions. First, data collection and analysis are described in Sections 2.2 to 2.4, capturing the distinctive dynamics and riding behaviors associated with high-performance motorcycles. Second, a novel cycle construction method for synthesizing representative driving cycles was introduced in Section 2.5. The method was tuned on key DC metrics, showing improved results over the conventional MCMC, as detailed in Section 3. Third, the development of the Sport Motorcycle Driving Cycle (SMDC) is presented in Section 4, achieving a relative error on vehicle energy consumption lower than 1 %. Sections 5 and 6 further discuss the implications of the findings and the final remarks.

## 2. Methods and data

### 2.1. Methodology

This study developed a synthetic driving cycle using a Markov Chain Monte Carlo (MCMC) approach, modified with incremental logic, as summarized in Fig. 1. The methodology consisted of three main phases.

First, data acquisition, comprehensive of the route and vehicle selection, driving data collection, and analysis. The data were collected using an instrumented motorcycle, as detailed in Section 2.2. The data were then processed and statistically analyzed to identify the key driving metrics that most quantify vehicle energy consumption, with a summary of the most relevant aspects provided in Section 2.4. Based on this analysis, speed, acceleration, and road slope were selected as variables for defining the states of the Markov model. These states represent all possible system configurations, and their transitions are expressed in the transitional probability matrix (TPM).

Second, the construction method was defined, including the Markov states definition, the TPM determination, and the parameter setting of the incremental method. The Markov model was calibrated and tuned by comparing the statistical difference between the synthetic speed profiles from long-run MCMC simulations and the reference dataset. The long-run MCMC result is shown in Section 3.1, and gives specific insights into the model. Through random walks, several state predictions were estimated and added

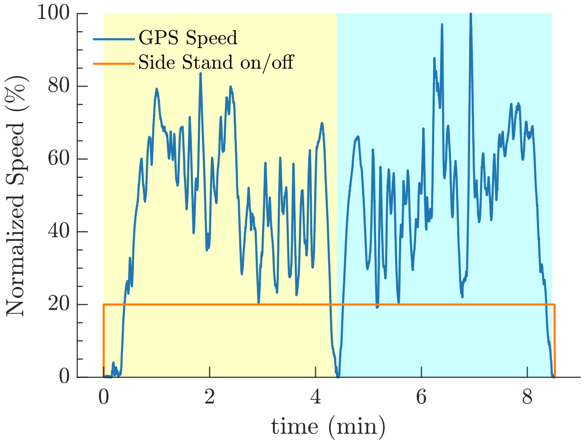


**Fig. 2.** Normalized speed profile of a key on/off event. The event was determined by the side stand closure. This event was compounded by two micro-trips, whose duration is shown by the highlighted areas.

to complete a single driving cycle. The incremental method, which combines different random walks, is introduced in Section 2.5, while minimizing the performance value between the synthetic and reference data.

Finally, the DC synthesis phase, where synthetic driving cycles were generated through incremental random walks. After processing, the speed profiles candidates were evaluated via the performance value, and only those with an error below a predefined threshold of 5 % were validated and accepted as a final, representative driving cycle.

The vehicle dynamics was modeled in Section 2.3, along with its characteristic parameter relationships. Based on this vehicle model, the energy consumption or mean tractive force ($\bar{E}_t$) was calculated. This energy is independent of the powertrain efficiency and depends only on the vehicle parameters, ensuring the same riding behavior regardless of the powertrain type. Vehicle energy consumption, defined as the energy consumed per unit distance (kWh/km), will subsequently be referred to simply as energy consumption and will assess the DC demand. The proposed DC construction method was then applied to real-world data in Section 4 to synthesize at least one representative speed profile, summarizing the overall driving data. Finally, the discussion and conclusions are presented in the corresponding sections.

### 2.2. *Driving data collection and processing*

Data were provided by Ducati Motor Holding S.p.a. and were recorded during a sport motorcycle road test. The dataset consisted of real-world telemetries of an instrumented sport internal combustion engine (ICE) motorcycle, a Ducati V2 Streetfighter with a maximum nominal power of 115 kW. The driver's path was the same for all three days to have a reference track to evaluate, as well as the vehicle setup. The trips were on extra-urban roads in central Italy, between hilly terrain, and not for commuting. The survey was conducted using dedicated riding tests with test pilots. Because of constraints on data collection and taking advantage of the numerous years of experience of the test drivers, the study concentrated on this route. The route consists of all extra-urban and hill sections of the road, taken at a reasonable pace, the same pace used for general assessment of dynamic motorbike behaviour and light stress testing. The data is the property of the collaborating company, and access was limited to strictly necessary information and limited in its sharing. The inertial measurement unit (IMU) and the GNSS unit acquired the vehicle's position and orientation. The speed signal and its derivative by time (acceleration) were recorded, together with CAN bus signals needed for the combustion management, such as the fuel rate, the motor speed, and the atmospheric temperature and pressure, via a dedicated acquisition system. The raw data were processed to reduce noise via a low-pass filter with a cut-off frequency of 2 Hz. The data with a bad GNSS signal were removed. Under these conditions ( the same route and motorcycles), the database was considered homogeneous and representative of a sport motorcycle tour on hilly extra-urban roads.

The speed profiles were divided into *key-on/off* events. These latter events were defined via the motorcycle turning on and side kickstand closure, while the events ended with the vehicle turning off or opening the side kickstand. An example of *key-on/off* event is shown in Fig. 2. From all the data, the complete (i.e., no missing speed signal) events were collected, for a total of 101 micro-trips and almost 387 km traveled.

The category of motorcycle establishes the maximum permissible limits for riding style, including factors such as top speed and peak acceleration. Factors such as road and traffic configurations, along with rider behavior, can only act to decrease the riding limits, affecting the transition probability matrix. Urban environments and heavy traffic conditions will lower the average speed, constraining the riding style. Therefore, it is essential to meticulously consider variations among roads, vehicles, and riders. If necessary, clustering techniques or manual selection should be employed to create a homogeneous dataset suitable for the application of the method proposed here.

**Table 2**
Motorcycle model and environment parameters from the company data and (Cossalter, 2006).

| Symbol | Value | Unit | Description |
|---|---|---|---|
| $m$ | 280 | $[kg]$ | Vehicle and rider mass |
| $A_d$ | 0.8 | $[m^2]$ | Front cross-section area |
| $C_d$ | 0.4 | $[-]$ | Drag coefficient |
| $c_{rr}$ | 0.013 | $[-]$ | Rolling resistance coefficient |
| $\rho_{air}$ | 1.226 | $[kg/m^3]$ | Air density |
| $g$ | 9.81 | $[m/s^2]$ | Gravitational acceleration |

## 2.3. Vehicle dynamics model and driving cycle metrics

In addition to the typical parameters adopted for DC evaluation (based on kinematics), vehicle dynamics was also considered to estimate the energy consumption at the wheel. This can be expressed by the Mean Tractive Force (MTF) as introduced by (Guzzella and Sciarretta, 2007) and described in Eq. (6). The Mean Tractive Force ($\bar{E_T}$) is the mechanical energy normalized by the distance (i.e., a force), which is also the energy at the wheel spent by the vehicle for following the speed profile during traction periods ($F_{trac} \geq 0$). The MTF was calculated using a one degree-of-freedom vehicle model describing only the longitudinal dynamics (Cossalter, 2006). Thus, the load transfer, the tire slip, and the suspension influence were neglected. This simple vehicle model is commonly used to predict energy consumption with acceptable accuracy. The driving force must be equal to the sum of the inertia force ($F_{\text{in}}$), tire rolling resistance force ($F_{rr}$), the aerodynamic drag ($F_{\text{air}}$), and the gradient force due to the road slope ($F_{\text{grade}}$). These forces are described in the following equations:

$$F_{\text{trac}} = F_{\text{in}} + F_{\text{rr}} + F_{\text{air}} + F_{\text{grade}} \tag{1}$$

$$F_{\text{in}} = ma \tag{2}$$

$$F_{\text{rr}} = \begin{cases} mgc_{\text{rr}} \cos\theta & if\ v \neq 0 \\ 0 & if\ v = 0 \end{cases} \tag{3}$$

$$F_{air} = \frac{1}{2}\rho_{\text{air}} C_{\text{d}} A v^2 \tag{4}$$

$$F_{\text{grade}} = mg \sin\theta \tag{5}$$

$$\bar{E_{\text{T}}} = \frac{\int_0^{t_{\text{trac}}} F_{\text{trac}}(\tau) v(\tau)\, d\tau}{\int_0^{t} v(\tau)\, d\tau} \tag{6}$$

where $m$ is the vehicle mass, $v$ is the vehicle speed, $a$ is the longitudinal acceleration, $\theta$ is the road slope angle, $c_{rr}$ is the rolling coefficient, $A$ is the frontal cross-section area, $C_d$ is the longitudinal drag coefficient, $\rho_{air}$ is the air density, $g$ is the gravitational acceleration, and the time $t$ is replaced by the dummy variable $\tau$ in Eq. (6). This substitution ensures the distinction between the variable of integration and the variable on which the integral depends. All the vehicle parameters and the air density were considered and kept constant during the simulations. Typical vehicle parameter values can be found in (Cossalter, 2006) and (Lot, 2021), together with further vehicle dynamics descriptions. Table 2 reports the values of the parameters utilized in Eqs. (1) to (5). The $\bar{E_T}$ was calculated by integrating Eq. (1), only for positive values of $F_{trac}$ and normalized by the distance traveled.

The road slope can be calculated by the altitude GPS signal and the vehicle speed (Jia et al., 2021), as follows:

$$\theta = \arcsin\left(\frac{\Delta H}{\Delta D}\right) = \arcsin\left(\frac{\Delta H}{v(t)\delta t}\right) \tag{7}$$

where $\theta$ is the road slope angle, $\Delta D$ is the distance traveled in the sample time period $\delta t$, and $\Delta H$ is the change of altitude.

Considering only positive traction force meant that all braking power was dissipated, as is coherent with the conventional motorcycle, although electric vehicles can potentially recover a significant amount of kinetic energy via regenerative braking (Gao et al., 1999). In the driving cycle, where the vehicle starts at rest and returns at rest (zero speed), there is a zero difference in kinetic energy. However, in the case of electric vehicles, only a portion of kinetic energy can be recovered due to the resistance and the non-unitary powertrain efficiency. This work focuses on obtaining equivalent driving cycles and not on specific powertrain performance; thus, only the mean tractive force was used to calculate the energy consumption. The tractive energy describes the energy demand at the wheel for conventional and electric vehicles, under the hypothesis of having the same kinematic and vehicle parameters. The adaptation to electric and hybrid systems should take into account both the energy at the powertrain and the energy recovery, as done in other work (O'Keefe et al., 2007). Intuitively, for a very high regenerative ratio, the inertia and potential energy may affect energy consumption with little relevance, and all the energy would be spent on rolling and aerodynamic resistance. In this situation, the aerodynamic speed would be a relevant metric, and consequently, the speed distribution. To obtain the same characteristic acceleration and aerodynamic speed with a DC facilitates the assessment of different powertrain systems, brake blending strategy, gear shifting, and more.

To validate the synthesized DCs, the Performance Value (PV) was used as a criterion (Hung et al., 2007), described in the Eq. (8); where $\psi_i$ is the i-th synthesized DC statistic (i.e., average speed), $\psi_t$ is the target or data value, and $W_i$ is the i-th element of the weight vector. The performance value ranked the constructed driving cycle candidates via the sum of the error between the DC statistic and the target values; ideally, the performance values should be zero. The performance values collected the error on different DC metrics. Although these metrics were based on the DC kinematic, they also have as good a correlation with power, fuel consumption, and exhaust gas emission for light vehicles as the Relative Positive Acceleration (RPA) (Ericsson, 1999). This type of correlation was also investigated for characteristic acceleration ($\tilde{a}$) as shown in Section 2.4. The RPA describes the amount of work needed to increase a mass unitary vehicle speed (kinetic energy), and it is normalized by the total distance, as defined in Eq. (9),

$$PV = \sum_{i}^{N} (|\psi_i - \psi_t| \cdot W_i) \tag{8}$$

$$RPA = \frac{\int_0^t a^+(\tau) \cdot v(\tau)\, d\tau}{\int_0^t v(\tau)\, d\tau} \tag{9}$$

where $a^+$ is the positive acceleration, and $v$ the vehicle speed. This parameter is defined only by the vehicle kinematics and serves as an indicator of the DC *dynamicity*; it is high when the power demand is high (Ericsson, 2001). A speed profile with 0.1 or lower RPA is considered a *soft* cycle (Giakoumis, 2017). The RPA metric can be used to compare the harshness of different cycles that have a similar average travel speed (Edwards, 2022). For example, the WMTC speed profile class 3, subclass 2 has RPA values of 0.20, 0.19, and 0.11 $m/s^2$, for parts 1, 2, and 3, respectively; while the experimental data RPA value was 0.71 $m/s^2$, more than three times the highest WMTC RPA value. This latter value by itself indicated a different riding behavior from the homologation cycle, characterized by a high *dynamism*. If the road slope is null, the RPA is equal to the characteristic acceleration ($\tilde{a}$), introduced to describe the positive work due to the increment of kinetic and potential energy (O'Keefe et al., 2007). Including the road slope, the data had a $\tilde{a}$ value of 0.749 $m/s^2$. The impact of air resistance on the vehicle can be described via the square of the aerodynamic speed ($V^2_{\text{aer}}$), and together with the characteristic acceleration, can describe the energy demand (O'Keefe et al., 2007). The $\tilde{a}$ and $V^2_{\text{aer}}$ are described by the following equations, respectively:

$$\tilde{a} = \frac{\int_0^t (a(\tau)v(\tau) + g\Delta H(\tau))^+ d\tau}{\int_0^t v(\tau)\, d\tau} \tag{10}$$

$$v^2_{\text{aer}} = \frac{\int_0^t v(\tau)^3 d\tau}{\int_0^t v(\tau)\, d\tau} \tag{11}$$

where $\Delta H$ is the elevation increment, and the superscript + means only the positive values are integrated over time.

The formulae introduced described a continuous function, and for implementing on the discrete data, a quasistatic approach was applied. This approach considers small time steps for which the speed, acceleration, and the road angle are constant over time (Guzzella and Sciarretta, 2007). Usually, the time intervals are all equal with a length of 1 second, and for short time intervals, the energy consumption is accurate (Guzzella and Sciarretta, 2007).

To build an equivalent vehicle energy demand, the vehicle rest can be neglected due to the zero mechanical energy demand in this situation, thereby excluding the powertrain and auxiliary power. In any case, the method introduced here can be applied to a generic set of CPs.

### 2.4. Data analysis

The high-performance motorcycle allows high acceleration as well as high deceleration. The riding behavior could be different compared to high-performance car driving, due to the possibility of filtering, overtaking, and higher acceleration. On urban roads, the vehicle speed is under limitations and affected by the presence of other vehicles, traffic lights, cross junctions, and other agents/infrastructures. The data shows a different riding style to the WMTC (Fig. 3a), with high acceleration (up to 8.5 m/$s^2$) and high deceleration (up to - 10.9 m/$s^2$). The average speed was 61.8 (km/h), the average driving speed was 67.44 (km/h), and the speed standard deviation was 31.3 (km/h). Neglecting idle time means focusing just on micro-trips. Even if the fuel performance is low when the vehicle rests, the absolute value of the fuel consumption is also low, and for an electric motorcycle, energy consumption is basically null. For the analysis, only the micro-trips longer than one km were considered, reducing the number of micro-trips from 101 to 86. A strong correlation was found between the average speed and the aerodynamic speed (0.96 Pearson coefficient), between the maximum speed and the aerodynamic speed (0.89), and between the aerodynamic speed and the speed standard deviation (0.9). These speeds were all strongly correlated, so just using one among them is sufficient. Fig. 3b shows the fuel performance ($\bar{F}$) vs the characteristic acceleration for micro-trips longer than one kilometer.

A linear fit based only on the characteristic acceleration obtains an $R^2$ of 0.82 with an RMSE of 2.05 km/l. Two models were constructed to predict $\bar{F}$ using only two cycle metrics. A two-layer neural network model (NN) and a Matern 5/2 Gaussian Process regression (GPR) model were trained on around 85 % of the data, after random data division for a 5 k-fold cross-validation. The other 15 % of the data (13 micro-trips) were used as a test after the training; the results are shown in Table 3. Figs. 3c and d show the fuel performance prediction using just the characteristic acceleration ($\tilde{a}$) and the aerodynamic speed ($V^2_{\text{aer}}$) by the NN model, and the GPR model, respectively. The GPR model was able to predict the fuel consumption with an $R^2$ equal to 0.95 and an RMSE of 1.18 km/l for validation data, while the NN model predicted $\bar{F}$ with an $R^2$ equal to 0.94 and an RMSE of 1.21 km/l for validation data. The

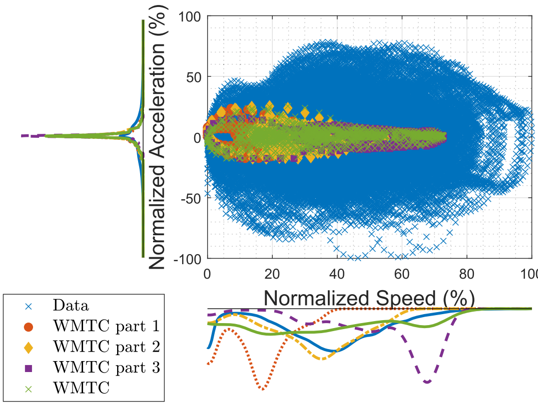


(a) SAPD comparison.

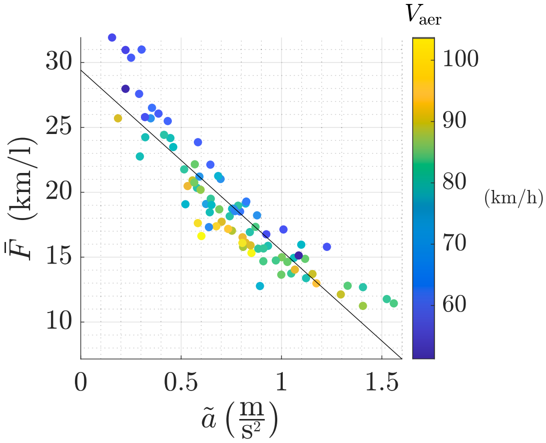


(b) Fuel performance linear regression.

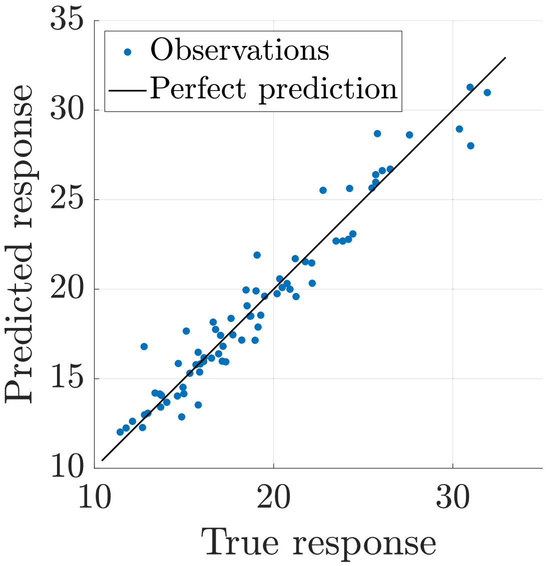


(c) Fuel performance prediction by neural network.

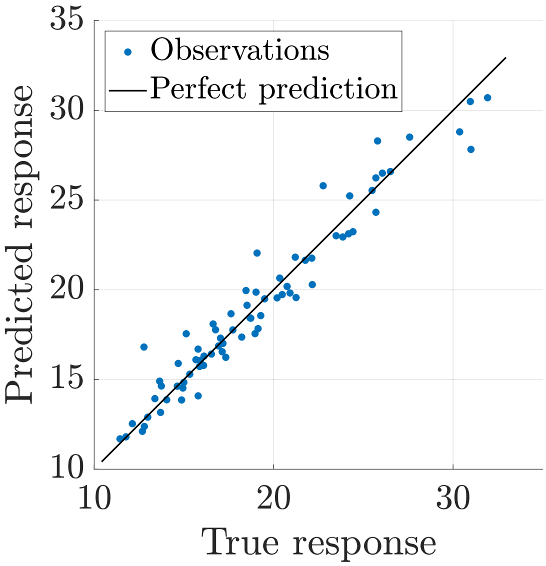


(d) Fuel performance prediction by Matern 5/2 GPR.

**Fig. 3.** a) Speed acceleration probability distribution, comparison between data and WMTC. b) fuel performance vs characteristic acceleration for all micro-trips longer than 1 km (86 out of 101). A linear fit obtained an $R^2$ of 0.82 and an RMSE of 2.05 km/l. The color indicates the aerodynamic speed magnitude; high values tend to lie below the line (worst fuel consumption), and low values tend to lie above. c) and d) show the fuel performance prediction using the characteristic acceleration and aerodynamic speed for a neural network (NN) and regression models. The regression model obtains an $R^2$ equal to 0.95 with an RMSE of 1.18 km/l, while the NN model obtains an $R^2$ equal to 0.94 with an RMSE of 1.21 km/l.

**Table 3**
Results of the neural network (NN) model and the Gaussian process regression (GPR) to predict the fuel performance.

| Model | Validation | | | | Test | | | | Training time |
|---|---|---|---|---|---|---|---|---|---|
| | RMSE | MSE | $R^2$ | MAE | RMSE | MSE | $R^2$ | MAE | (sec) |
| Neural Network | 1.21 | 1.47 | 0.94 | 0.90 | 1.69 | 2.85 | 0.81 | 1.19 | 1.94 |
| Matern 5/2 GPR | 1.18 | 1.39 | 0.95 | 0.85 | 1.63 | 2.66 | 0.82 | 1.17 | 2.76 |

testing results show a lower performance of the models, but with a still significant correlation ($R^2 > 0.8$) and lower RMSE than the linear regression.

It is noteworthy that fuel performance ($\bar{F}$) can be predicted with high accuracy even without vehicle parameters. The two characteristic parameters were also able to capture the average engine power (clutch torque times engine speed) delivered in the micro-trips; indeed, a linear fit obtained an $R^2$ equal to 0.92 and an RMSE equal to 1543 W. The average negative engine power was still well fitted by a linear relation on characteristic acceleration, and the aerodynamic speed with a $R^2$ equal to 0.78 and an RMSE of 884 W.

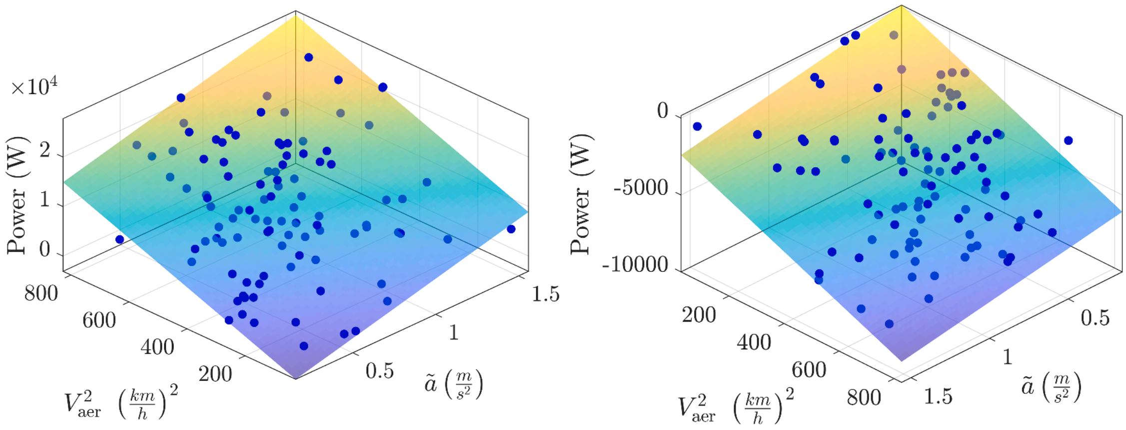


(a) Positive power (b) Positive power

**Fig. 4.** a) Shows the average engine positive power vs the characteristic acceleration $\tilde{a}$ and the aerodynamic speed ($V_{aer}$). These two latter parameters were able to capture the positive power, a linear fit obtained an $R^2$ of 0.92 with an RMSE of 1543 W. b) shows the average negative engine power, with an $R^2$ equal to 0.78 and an RMSE of 884 W.

Figs. 4a and b show the average positive and average negative power vs the characteristic acceleration ($\tilde{a}$) and the aerodynamic speed ($V_{aer}$). The Pearson correlation between the average engine power and the aerodynamic speed was 0.82 (high correlation), and the correlation between the former power and the characteristic acceleration was 0.66 (moderate correlation). Even if high accelerations are more common at low speeds (high gear ratio), the power delivered at low vehicle speeds is generally lower than at high speeds. In this latter situation, the power delivered is dissipated primarily to counteract the aerodynamic drag, and the possible acceleration is low and becomes null at the maximum vehicle speed.

### *2.5. Driving cycle construction method*

The method developed and proposed here is based on a Markov Chain Monte Carlo (MCMC) approach already used, and modified by the authors to reduce the performance value (PV) or residuals at zero. The MCMC method was already successfully applied for the synthesis of driving cycles after defining the Markov states by longitudinal speed and acceleration (Lee and Filipi, 2011; Silvas et al., 2016; Esser et al., 2018). The MCMC method implemented in this work was based on a discrete-time and time-homogeneous Markov chain model (DTHMC), which is a sequence of random variables (stochastic process), with the Markovian property, also known as the memoryless property. This latter property can be summarised as the state at any given time ($i_n$) gives all information about the past, and it is the only one relevant to the future state ($i_{n+1}$). Namely speaking, the past outcomes of the stochastic process do not influence the next outcome. A mathematical description is given as follows:

$$\mathrm{P}(X_{n+1} = i_{n+1} \mid X_n = i, X_{n-1} = i_{n-1}, \dots, X_0 = i_0) = \mathrm{P}(X_{n+1} = i_{n+1} \mid X_n = i) \tag{12}$$

where $\{X_n,\ n = 0, 1, \dots\}$ indicates the random variable at the time $t = n$, and the set of possible values that it can take is the state space. The state space was defined by vehicle dynamics, discretization of speed, acceleration, and road slope. Fig. 5b shows the state space definition in the speed-acceleration plane. The notation $p_{ij}$ indicates the transition probability of transferring from state $i$ to state $j$ in one time step; for the mathematical meaning, see Eq. (13). The transition probabilities between all the states can be rewritten in a matrix form, called the Transition Probability Matrix (TPM). The evolution of the Markov chain is determined by the transition probability matrix given the initial state $X_0$.

$$p_{ij} = \mathrm{P}(X_{n+1} = j \mid X_n = i) \tag{13}$$

After constructing the TPM, speed time series can be obtained by simulating the Markov Chain state walk, namely a random walk through a sequence of the MC states. The random walks were simulated in MATLAB based on a uniform probability distribution and the Monte Carlo approach. To construct the TPM, the states or classes must be defined via physical signals. In this work, the classes were defined by the longitudinal velocity ($v$), acceleration ($a$), and road slope ($\theta$) after their discretization via constant delta values. Figs. 5a and b show an example of a 3D Markov Chain model for only three states, and speed-acceleration space discretization, respectively.

A fine mesh to determine the states was implemented in this work, comprising 192591 states. Acceleration, speed, and road grade delta step were 0.18 ($m/s$), 0.1 ($m/s^2$), and 0.1 ($\circ$), respectively. The time step was 0.1 s. The mesh was sized as a trade-off between a good vector space discretization (needed due to the high sport motorcycle acceleration) and the computational time and memory needed for synthesis. Indeed, the TPM has as many elements as the states squared. As shown in Fig. 5b, some states were physically meaningless and thus avoided their definition, such as those above the maximum power. Instead of defining all the possible states, only the states that occurred at least once were implemented to construct the TPM. A non-homogeneous distributed mesh that collects

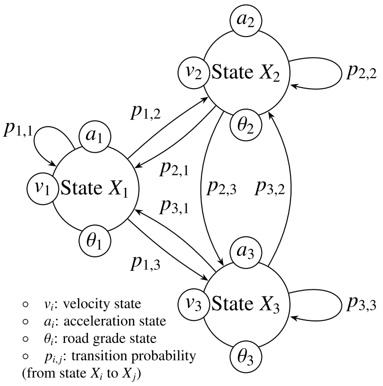


(a) Markov Chain

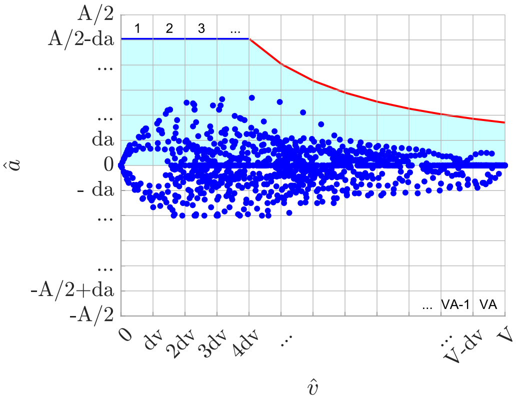


(b) Speed-acceleration speed discretization.

**Fig. 5.** a) Markov chain illustration for 3 states (speed, acceleration, and road slope), adapted from (Topić et al., 2020). b) Example of the speed-acceleration space discretization. The first three states are indicated in the top left corner by numbers 1, 2, and 3. The highlighted area (cyan) represents the achievable classes for the vehicle; the top blue line indicates the wheelie limit, and the red line indicates the maximum power limit. WMTC operating points are also shown (blue dots). (For interpretation of the references to colour in this figure legend, the reader is referred to the web version of this article.)

the difference in energy consumption might be used to reduce the number of states or the error introduced by the discretization. The new process proposed in this work was based on an *incremental* method that combines random walks iteratively, while minimizing the error on the performance value. The initial state ($v(0) = 0$, $a(0) = 0$, $\theta(0) = 0$) was chosen, and one random walk was performed. The last state obtained was set as a new beginning state, and a finite number ($n_i$) of random walks of the same length ($l_i$) were synthesized. The procedure is shown in Fig. 6a. The random walk quantity and duration might be different for each iteration, but fixed values for both parameters ($n_i$, $l_i$) were chosen. Among all the outcomes simulated, the random walk, added to the previous part, that most reduced the performance value was selected, as shown in Fig. 6b. The procedure at the next time step was repeated, setting the initial state equal to the last one selected.

The speed profile building and combining was continued until the error was lower than or equal to a threshold or the iteration was higher than the maximum set. An example of residual minimization is shown in Fig. 6c. The final driving cycle was obtained as a union of shorter random walks, selected to minimize the residual step-by-step. In other building methods, the duration was chosen in advance for arbitrary reasons, while in this way, the length is a function of the error.

### 2.6. *Driving cycles validation*

The speed profiles built were processed via a low-pass filter to remove the stair value introduced with the discretization, and the synthetic driving cycle metrics were extracted. The longitudinal acceleration was then computed as the speed derivative over time, and the set of metrics that form the performance value was extracted by the synthesized cycles. Prediction of fuel consumption to validate the results was obtained by a regression model or training neural network, given a synthetic speed profile (Nyberg et al., 2014; Topić et al., 2021). In this work, the focus was on the mechanical energetic demand to mimic the same riding style independently of the powertrain nature; thus, the mean traction force ($\bar{E}$) was calculated by the vehicle model of Section 2.3.

The PV used in Section 4 for the synthesis of the driving cycles was defined as the weighted sum of the speed and acceleration distribution as follows:

$$PV = \sum_{i=1}^{n} |(v_{\text{sim}}(i) - v_{\text{data}}(i)) \cdot w_{\text{v}}(i)| + \sum_{i=1}^{n} |(a_{\text{sim}}(i) - a_{\text{data}}(i)) \cdot w_{\text{a}}(i)| \tag{14}$$

where $v_{\text{sim}}$ and $a_{\text{sim}}$ are the velocity and acceleration distribution of the simulated DC, $v_{\text{data}}$ and $a_{\text{data}}$ are the data speed and acceleration distribution, $w_{\text{v}}$ is the weight vector for the speed, and $w_{\text{a}}$ is the weight vector for acceleration. The speed was discretized in 19 bins from 0 to 190 km/h with a step of 10 km/h, a sufficient top speed to cover also other applications such as riding outside of regular roads. The acceleration counted 22 bins from -11 to 11 m/$s^2$ with a 1 m/$s^2$ step. The velocity and acceleration step values were similar to other studies (Bhatti et al., 2021; Kamel and Huzayyin, 2024; Lee et al., 2025). The weight for the speed was defined as: $w_{\text{v}}$ = [0 0 1 1 1 1 1 1 1 1 1 1 1 1 0 0 0 0 0], and the weight for the acceleration as: $w_{\text{a}}$ = [0 0 0 1 1 1 1 1 1 1 1 1 1 1 1 1 1 1 0 0 0 0 ]. The weights were selected to cover at least 80 % of the data, resulting in an actual coverage of 86.6 % of the data SAPD. The $w_{\text{a}}$ is not symmetric like the bin acceleration classes because of the possibility of harsher deceleration. The selection of bin discretization influences the method's convergence. Specifically, a rough discretization tends to reduce the relative error at the cost of potentially more differences between the data and the synthesized DCs on the SAPD distribution. On the other hand, a fine discretization may fail to achieve convergence or may require additional iterations, resulting in failing or longer DCs.

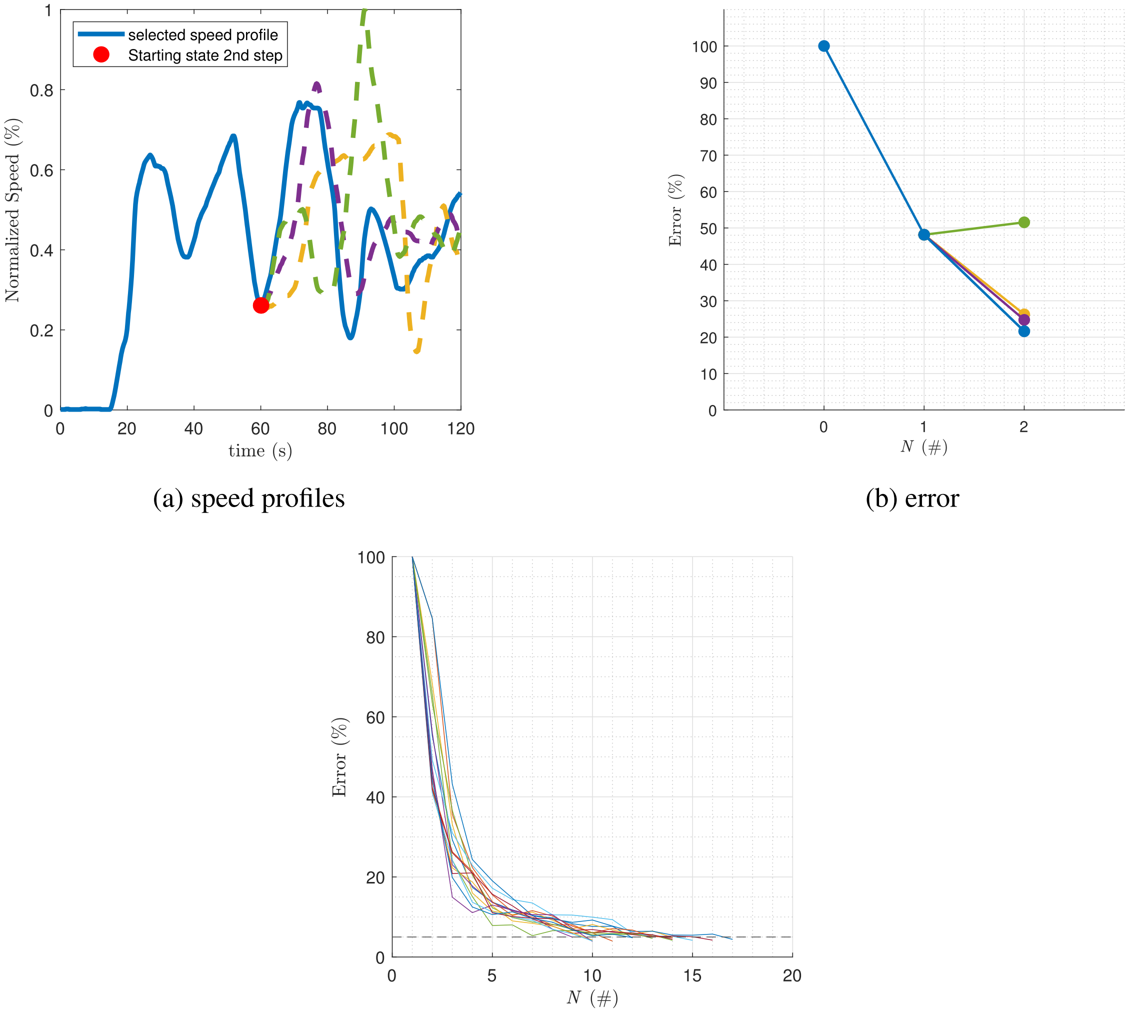


(a) speed profiles (b) error

(c) runs

**Fig. 6.** Evolution and selection of the speed profiles (a). The blue line had the lowest error among the other random walks (b). c) shows 15 runs that have a value equal to or lower than the error threshold (5 %). (For interpretation of the references to colour in this figure legend, the reader is referred to the web version of this article.)

The incremental method terminates the cycle construction when the PV error falls below 5 %, and only those DCs with a relative error in the sum of $\bar{E}$ and $\tilde{a}$ lower than 1 % were validated. Then, many decisions can be made to choose a representative cycle, like the one with the lowest absolute error or the shortest one. The final selection for the cycle developed is discussed in Section 4.

## 3. Incremental MCMC method performance

### 3.1. Long-run Markov model result

A *sufficiently* long random walks have the same data distribution. An irreducible aperiodic chain will reach its steady-state distribution ($\pi$) in an amount of time (or steps) called the mixing time. For evaluating the density mesh goodness (discretization size), long runs were used (30 times the data length). The synthesized speed profiles were then filtered to smooth the discontinuity derivation due to the discretization process. The incremental method was not applied to synthesize these long runs, because here the mesh density was investigated (i.e., state quantity) to represent the original data. A comparison of 9 features between the data and simulated speed profiles was reported in Table 4. Where $v_{\text{avg}}$ is the average speed, $v^{+}_{\text{avg}}$ is the average positive speed (that is, v > 0), $\sigma_v$ is the velocity standard deviation, $\sigma_a$ is the acceleration standard deviation, max speed is the maximum speed value, $a^{+}$ is the highest positive acceleration value and $a^{-}$ is the lowest negative acceleration value. The relative error between the long run and data was lower than 1 % across the features, indicating effective discretization, and the TPM successfully modeled the data.

**Table 4**
Relative error (%) between long run and data.

| $v_{avg}$ | $v^{+}_{avg}$ | $\sigma_v$ | $\sigma_a$ | $v_{max}$ | $a^{+}_{max}$ | $a^{-}_{min}$ | RPA | $\tilde{a}$ |
|---|---|---|---|---|---|---|---|---|
| -0.31 | -0.15 | 0.06 | 0.44 | -0.03 | -0.13 | 0.86 | -0.15 | 0.73 |

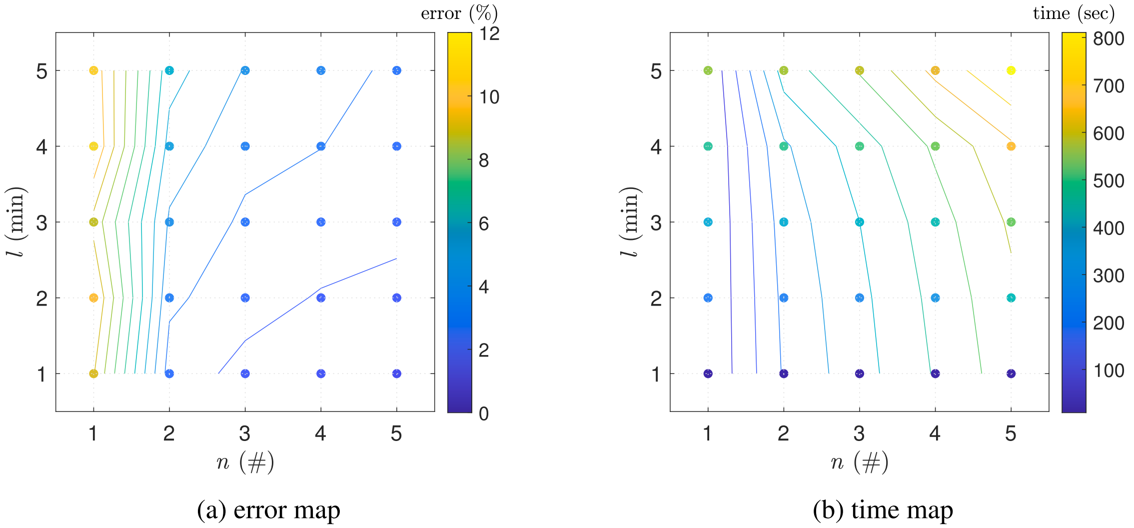


**Fig. 7.** Relative error (a) and computing time (b) maps of the incremental MCMC method. The speed profile length was constant (120 min), and both the number of random walks for step ($n$) and the length of a single simulation ($l$) were changed. The dots are the numerical values, while the lines are the isoerror/time values calculated by data interpolation.

### 3.2. *Incremental MCMC and MCMC comparison*

The comparison between the incremental MCMC and the MCMC was done for a fixed DCs duration of 120 min. The length of the single simulation ($l_i$) and the number of simulations ($n_i$) were kept constant for each iteration; thus, from now on, the time subscript $i$ is omitted. For each configuration of $n$ and $l$, 10 driving cycles were synthesized, for a total of 250 DCs. When $n$ was equal to one, there was no difference between this method and conventional MCMC, independently of the $l$ value. The variables $n$ and $l$ spanned from 1 to 5, representing the count of random walks and min, respectively, each increasing by one unit step. The mean relative error from the data and the mean computing time are shown in Fig. 7.

The lowest error was 1.53 % for $n=5$, and $l=1$ or point (5,1). The highest computing time was 810 s for point (5,5), and the lowest value was 8.9 s for point (3,1). The relative error was reduced by an $n$ increment and became higher with an $l$ increment as shown by the isoerror line in Fig. 7a. Increasing the parameter $l$ at a low value of $n$ did not influence the error as much as at a high $n$ value. An increment of $n$ or $l$ meant an increment in the computing time as shown in Fig. 7b. At low values of $n$, an increment of the other parameter took less time to compute than at higher values.

## 4. Sport motorcycle driving cycle development

The method described in Section 2.5 was applied to real-world data from Section 2.2. The speed profiles were recorded via GNSS and differentiated by time to obtain the longitudinal vehicle acceleration. Data with missing speed values were excluded. These data were processed, and the DC features were extracted.

Three hundred DCs were synthesized via the incremental MCMC method with a 5 % relative error on the PV. The error was computed as the weighted difference in speed and acceleration distribution as described in Section 2.6. Energy consumptions were obtained via the vehicle model for each speed profile. Only the DCs with an error on $\tilde{a}$ and energy consumption ($\bar{E}_T$) lower than 1 % were considered valid. Applying these criteria, just 11 of 300 cycles were validated (3.7 %). Differences between the data and the mean value of all cycles (300) and the validated cycles (11) are reported in Table 5, with the WMTC values as reference.

The $\tilde{a}$ relative error between the data and the average validated DCs was practically null. The $\bar{E}_T$ was 81.3 and 81.33 Wh/km for the data and the validated DCs, respectively, and was calculated via Eq. (6). The WMTC differs significantly from the data, highlighting that a proper cycle is necessary for a good driving representation. The average distance was 49.59 km and 56.32 km for the synthetic and validated speed profiles, respectively. The time ranged from 31 to 76 min. Among the speed profiles validated, the Sport Motorcycle Driving Cycle (SMDC) was selected and is shown in Fig. 8, including elevation. The SMDC was chosen because it was the shortest DC among the validated DCs, with initial and final speeds close to or equal to zero, and a net elevation close to zero.

**Table 5**
Comparison between data, approval cycles, and synthesized driving cycle average results.

| Cycles | $\mathbf{v}_{avg}$ $\left(\frac{km}{h}\right)$ | $\mathbf{v}^{+}_{avg}$ $\left(\frac{km}{h}\right)$ | $\boldsymbol{\sigma}_{v}$ $\left(\frac{km}{h}\right)$ | RPA $\left(\frac{m}{s^2}\right)$ | $\tilde{\mathbf{a}}$ $\left(\frac{m}{s^2}\right)$ | $\bar{\mathbf{E}}_{T}$ $\left(\frac{Wh}{km}\right)$ | Distance (km) |
|---|---|---|---|---|---|---|---|
| Data | 61.80 | 67.44 | 31.30 | 0.705 | 0.749 | 81.30 | 387 |
| Synthetic DCs | 61.31 | 66.94 | 31.11 | 0.696 | 0.745 | 81.64 | 49.59 |
| Validated DCs | 61.86 | 67.33 | 30.79 | 0.703 | 0.749 | 81.33 | 56.32 |
| WMTC part 1 | 24.39 | 29.93 | 16.68 | 0.196 | – | 26.23 | 4.07 |
| WMTC part 2 | 54.67 | 59.21 | 25.06 | 0.188 | – | 37.71 | 9.11 |
| WMTC part 3 | 94.42 | 97.17 | 30.54 | 0.117 | – | 59.74 | 15.73 |
| WMTC | 57.83 | 64.01 | 37.88 | 0.154 | – | 48.09 | 28.91 |

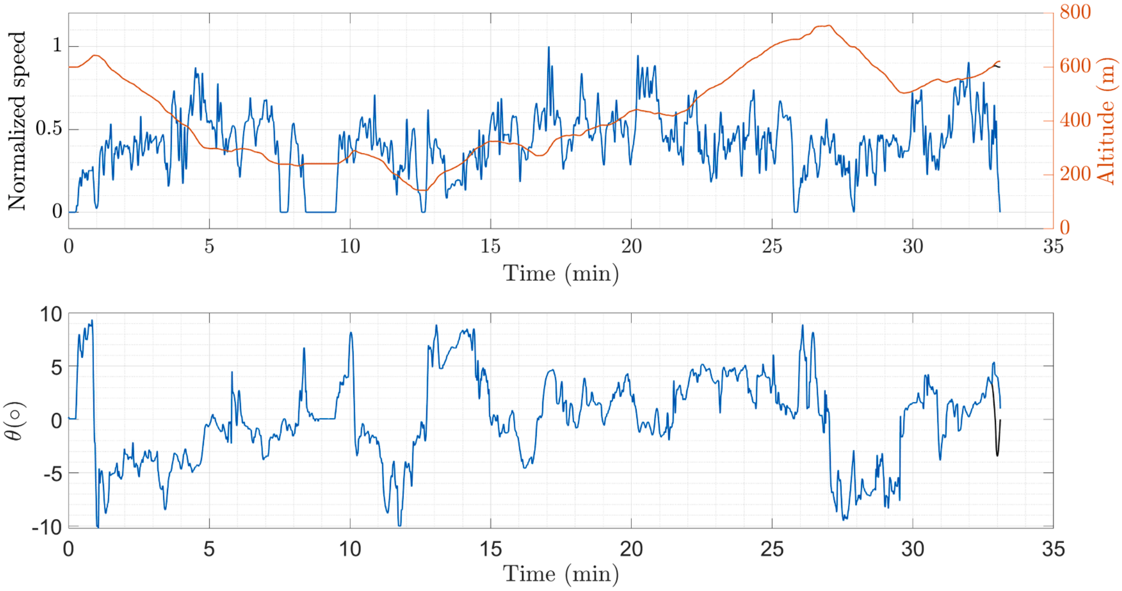


**Fig. 8.** Shows the Sport Motorcycle Driving Cycle (SMDC) speed values and elevation on the top plot, and the road grade on the bottom plot. On black, the slight road slope modification to obtain a zero net altitude. The relative errors were 2.1 %, -0.55 %, -0.4 %, and -0.31 % for the positive average speed, RPA, $\tilde{a}$, and $\bar{E}_T$, respectively. The duration was almost 33 min.

The Sport Motorcycle Driving Cycle has an average velocity equal to 64.95 km/h, an average driving speed of 68.82 km/h, a speed standard deviation of 29.88 km/h, and a duration of 33.1 min. Although good results were obtained by the driving cycle, the net altitude was positive (21.43 m), and repeating this cycle several times to estimate the driving range or the emission will result in a gain of altitude. Thus, the last 20 s of the slope were modified to achieve a net zero altitude. Similarly, the driving cycle must end with zero speed, reducing the number of candidate speed profiles. The road slope was changed using a spline, resulting in a net altitude equal to -5.1 $10^{-4}$, which is negligible. Adjusting the road slope reduced the characteristic acceleration to 0.746 m/s$^2$, and decreased $\bar{E}_T$ to 81.05 Wh/km, with relative errors to the data of -0.4 % and -0.31 %, respectively. Table 6 reports the comparison between the data and the SMDC for 12 characteristic parameters.

The vehicle power distribution, calculated via the model of Section 2.3, for the Sport Motorcycle Driving Cycle and the data is shown in Fig. 9a, while Fig. 9b shows the difference in the SAPD between the data and the SMDC, resulting in a root sum squared difference of 6.51.

The maximum power is 66.57 kW, the minimum is -61.73 kW, the average power is 1.97 kW, the median power is 1.18 kW, and the standard deviation is 11.2 kW. The difference in power between the SDMC and the driving cycle without altitude correction is only in the last 20 s. The road slope was reduced to obtain a net zero altitude to balance the 21.43 m of altitude gain at every cycle. Reducing the road slope meant reducing the power in the last part of the cycle, with a maximum difference of -775.2 W.

## 5. Discussion

The study collected 387 km of sport motorcycle riding. The data analysis highlights that characteristic parameters differ significantly from type approval driving cycles, especially in dynamics related indicators, like the RPA and $\tilde{a}$. Furthermore, the WMTC does not consider elevation changes, which are crucial for correct energy and emission estimation. The correlation analysis showed the importance of the characteristic acceleration ($\tilde{a}$) and the aerodynamic speed ($V^2_{\text{aer}}$) to predict the fuel performance accurately, with

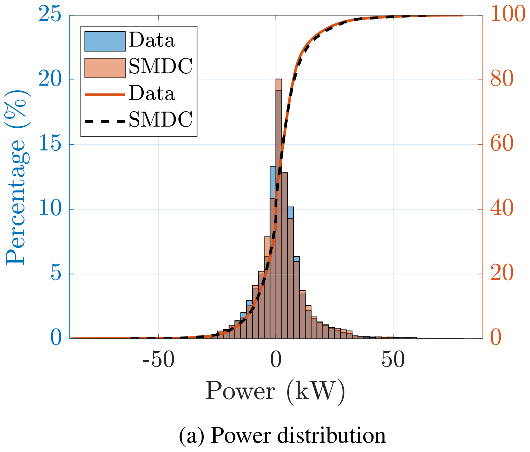


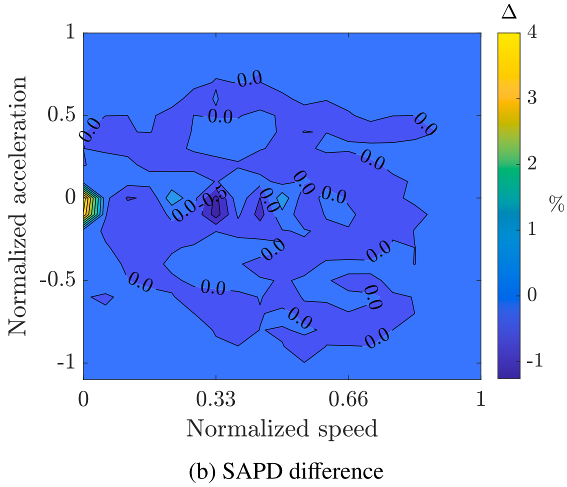


**Fig. 9.** a) Shows the vehicle power distribution percentage on the left y-axis, and the cumulative density function on the right axis for the data and the SMDC. The power was calculated by the model introduced in Section 2.3. b) shows the difference between the data and SMDC speed acceleration probability distribution (SAPD), with a root sum square difference of 6.51.

**Table 6**
Characteristic parameters (CPs) comparison between data and SMDC.

| Group | CP | Description | Unit | Data | SMDC |
|---|---|---|---|---|---|
| Speed related | $v_{avg}$ | average speed | $\frac{km}{h}$ | 61.80 | 64.95 |
| | $v^+_{avg}$ | avg. running speed | $\frac{km}{h}$ | 67.44 | 68.82 |
| | $\sigma_v$ | std. of speed | $\frac{km}{h}$ | 31.3 | 29.88 |
| Acceleration related | $a^+_{avg}$ | avg. positive acceleration | $\frac{m}{s^2}$ | 1.20 | 1.29 |
| | $a^-_{avg}$ | avg. negative acceleration | $\frac{m}{s^2}$ | -1.39 | -1.44 |
| | $\sigma_a$ | std. of acceleration | $\frac{m}{s^2}$ | 1.81 | 1.82 |
| Time related | % $t_{running}$ | % of time running | – | 91.36 | 94.38 |
| | % $t_{idling}$ | % of time idling | – | 8.64 | 5.62 |
| | % $t_{accelerating}$ | % of time accelerating ($> 1m/s^2$) | – | 22.59 | 22.87 |
| Dynamic related | $\tilde{a}$ | characteristic acceleration | $\frac{m}{s^2}$ | 0.749 | 0.746 |
| | RPA | relative positive acceleration | $\frac{m}{s^2}$ | 0.705 | 0.701 |
| | $V^2_{aer}$ | aerodynamic speed | $\frac{m^2}{s^2}$ | 510.97 | 526.17 |

an RMSE of 1.21 and 1.18 km/l for the NN and regression models, respectively. The $\tilde{a}$ and $V^2_{aer}$ also correlated very well with the average positive and negative micro-trip power.

The Markov chain model constructed allowed for successful *mimicking* the data via random walks. The relative error between the synthetic speed profile and the data for all nine features shown in Table 4 was lower than 1 %. A fine mesh (high discretization) and a short time step (0.1s) were able to catch the steepest acceleration (typical of sporty driving), and the relative error on the maximum and minimum acceleration values was low (0.86 %, -0.13 %).

A long-run evolution of a Markov chain could capture even better the statistical value of the data, which is not guaranteed on a short walk. The mesh and delta time tuning settled the minimum error achievable by a long run, although the RAM required increases with the number of states, and the time to construct a cycle increases with a lower time step.

The incremental MCMC applied to driving cycles synthesis had a lower error than the conventional MCMC procedure for the same DC length, as shown in Fig. 7a. Resulting in more efficient driving cycles. The point with coordinate (1, 1) was equal to the conventional MCMC method. Vice versa, for the same length of MCMC and incremental MCMC, the latter will have a lower error on average. This result was obtained despite an increase in computing time. The time required for constructing the speed profile depends on the computer settings and the code efficiency. Thus, instead of focusing on the absolute value, it is preferable to look at the difference in computing time. Changing $n$ for the same $l$ increases the time needed for the construction, albeit there was an exception for $l$ equal to 1. Moving on the y-axis in the error maps meant a higher increment than moving along the x-axis. The highest relative error was 10.9 %, point (1,4), and the lowest was 1.5 % for the point of coordinates (5,1). An increment of $l$ also means an increment in the relative error, while an increment of $n$ corresponds to an error reduction. On these considerations, for saving time is better to have the higher value of $n$ and the lowest value of $l$ that matches the error value needed.

Error minimization is not always guaranteed, and the method applied for the synthesis of motorcycle speed profiles nevertheless achieved good results, especially for the validated cycles. The method, due to its coherence between starting data and synthesized

DCs, is potentially suitable for a broad range of scenarios, and even a formal analysis might be performed to generalize the method. The 11 out of 300 DCs speed profiles validated had a sum of $\tilde{a}$ and $\bar{E}$ lower than or equal to 1 %. Moreover, the length of the DCs is not determined; instead, the construction continues until the error meets or drops below a specific threshold. On average, the incremental method *mimics* the data behavior, as shown in Table 5. The ratio of cycle validation success was 11 on 300 (3.7 %). A higher threshold error will result in more possible candidate cycles, but with a higher difference between the reference data. The validated driving cycle mean tractive force ($\bar{E}$) was practically the same as the data.

The Sport Motorcycle Driving Cycle (SMDC) achieved an error in $\bar{E}$ and $\tilde{a}$ very low, of -0.31 % and -0.40 %, respectively. Furthermore, the SMDC includes the road slope, even if the last 20 s were modified to reach a zero net altitude, not to gain altitude by repeating the cycle. The driving speed is higher than the reference data (2.1 %), still resulting in an acceptable error. Noteworthy was the short SMDC duration, 35.8 km, almost 33 min, corresponding to a reduction of -90.7 %.

As shown in Fig. 3a, the highest speed value occurred with a very low frequency. Neglecting the highest speed values via the weight in Eq. (14) did not significantly influence the overall speed behavior and allowed for a reduction in the driving cycle length. Omitting these extreme values had minimal impact on energy consumption; it reduced the absolute maximum power. However, the maximum power required for a motorcycle is set by the top speed on a flat road, as specified in the design.

In conclusion, a fine mesh (low discretization of state space and time) and the incremental MCMC method were applied to real-world data to construct at least a synthetic speed profile with an error on $\bar{E}$ lower than 1 %. Despite the good results of the methods, a proper driving cycle should conclude with a zero speed and zero net altitude to not gaining kinetic or potential energy by repeating it, reducing the number of possible candidates. Thus, some slight processing might be needed after the cycle construction. The method requires time (several minutes) to compute the cycle on a personal computer of average specifications (Intel i7-12700, 16 GB RAM), which is not a problem in an offline speed prediction, as in the case of DC development. Furthermore, the speed statistical behavior can be collected in the TPM rather than from all the telemetry data.

## 6. Conclusion

The study quantifies the discrepancy between real-world riding and the approval cycle, showing that the WMTC does not adequately capture the dynamics of high-performance motorcycles. Differences in characteristic parameters, such as RPA, exceed a factor of three. By collecting and analyzing real-world data via a sport motorcycle, a novel Sport Motorcycle Driving Cycle (SMDC) was developed using the Markov Chain Monte Carlo method, with modifications introduced here, and called the incremental MCMC, based on vehicle-independent metrics. The resulting SMDC achieved a high level of accuracy, with a deviation of only -0.31 % in energy consumption at the wheel, with -90.7 % length reduction.

The high discrepancies between real-world data and the type approval driving cycles underscore the need for cycle development that considers vehicle segmentation, particularly by engine size and usage context. Indeed, part of the WMTC and other motorcycle DCs were built on several motorcycles, mainly of small power. Furthermore, the standard DC does not include the road slope, which is essential for predicting fuel performance, as indicated by the results of the data analysis. In this regard, the SMDC represents a step toward more realistic and representative driving cycles for powerful motorcycles operating under sport-duty conditions. The higher vehicle-specific power observed in the SMDC compared to type approval cycles suggests that current homologation protocols may not adequately reflect real sport riding conditions. Consequently, there is a risk that sport motorcycles are being certified under driving cycles that significantly underestimate real-world fuel consumption and emissions.

From a methodological perspective, this work introduces a novel synthesis technique based on Monte Carlo Markov Chain modeling and incremental random walks. This approach enables the construction of driving cycles with reduced error rates, albeit at the cost of increased computational time. The study found that 3.7 % of the generated cycles met the dual criteria of brevity and accuracy, reinforcing the need for multiple iterations and selective validation when applying the method. Nevertheless, the approach is well-suited for offline driving cycle generation, where processing time is less critical than accuracy. The method might be applied to other case studies, and it is publicly available at the link in the dedicated section.

Among all the metrics describing a driving cycle, the characteristic acceleration ($\tilde{a}$) and the aerodynamic speed ($V_{aer}$) were found to be robust indicators of the fuel performance (km/l) and the average engine power, for micro-trips longer than 1 km. These latter two indicators estimated the fuel consumption with good accuracy, as well as the engine power. Consequently, energy and power can be described using only two parameters. The data analysis shows that the road slope was influential on consumption, and the characteristic parameters differed significantly from the WMTC, indicating a different riding behaviour.

While the study focuses on conventional engine motorcycles, the implications might be extended to the future development of electric sport motorcycles. The hypothesis posited that the performance of motorcycle riding is influenced more by attributes such as maximum power or wheelie limit rather than the specific type of powertrain employed. Due to the difference in powertrain, the riding style could be different. In the case of cars, for example, it was found that the EVs have higher dynamics, with higher acceleration and deceleration (Ye et al., 2023); however, for the case study here described, the high performances highlighted suggest that little margin for increase just due to the powertrain type is possible, since motorcycles are affected by wheelie and stability limits. Thus, the SMDC is a valid representation of ICE MC sport riding and sets the basis for sport EM design. In addition, the method may be extended to other vehicles like cars or more case studies.

Although the CO and NOx emissions were not collected, the vehicle-specific power is a crucial predictor (Park et al., 2023), and this latter power was higher than the standard cycles. The study shows that, at least in this case, the present conventional sport motorcycles are likely homologated using an unrepresentative driving cycle for sport riding. Thus, the clustering of vehicles by size and usage should be institutionalized within the regulatory framework for the development and homologation of the driving cycle. This would enable more precise classification and testing protocols that accurately reflect actual use cases.

Finally, the dataset used in this study covers a relatively short distance (387 km) and does not include direct emissions data such as CO and NOx. Future research should incorporate longer routes, different road topologies, more motorcycles, and integrate emissions measurement to validate and extend the current findings. The study gives hints on the reevaluation of current driving cycle standards used in the type approval of sport motorcycles, potentially leading to revised regulations that ensure consistency between certified and real-world performance, including fuel or electric energy consumption assessment. At the end, the SMDC is a new tool for sport motorcycle design, both ICE and electric.

## Open-source and data availability

The dataset used is confidential, while the code developed and used in this work is publicly available at this GitHub repository: https://github.com/A-Niccolai/Driving_Cycle

## CRediT authorship contribution statement

**Adelmo Niccolai:** Writing - original draft, Visualization, Software, Methodology, Investigation, Formal analysis, Data curation; **Lorenzo Berzi:** Writing – review & editing, Visualization, Validation, Methodology, Formal analysis, Conceptualization; **Niccolò Baldanzini:** Writing - review & editing, Supervision, Project administration, Methodology, Funding acquisition, Formal analysis.

## Data availability

The data used in this study are confidential.

## Declaration of competing interest

The authors declare that they have no known competing financial interests or personal relationships that could have appeared to influence the work reported in this paper.

## Acknowledgement

This work was supported by the Italian Ministry of Education, University and Research under Decree No. 1061 of August 10, 2021, which allocates resources from the PON “Research and Innovation 2014–2020” program for the activation of PhD courses within Action IV.4 “Doctoral programs and research contracts on innovation topics” and Action IV.5 “Doctoral programs on green topics. The authors express their gratitude to Ducati Motor Holding S.p.A. for providing access to the data.

## References

ACEM - European Association of Motorcycle Manufacturers, 2021. Decarbonisation of transport: powered two-wheelers (PTWs) on the road to 2050. https://www.acem.eu. ACEM Position Paper.

Adak, P., Sahu, R., Elumalai, S.P., 2016. Development of emission factors for motorcycles and shared auto-rickshaws using real-world driving cycle for a typical indian city. Sci. Total Environ. 544, 299–308. https://doi.org/10.1016/j.scitotenv.2015.11.099

André, M., 1996. Driving cycles development: characterization of the methods. In: International Fuels & Lubricants Meeting & Exposition. SAE International. https://doi.org/10.4271/961112

André, M., 2004. The ARTEMIS European driving cycles for measuring car pollutant emissions. Sci. Total Environ. 334–335, 73–84. Highway and Urban Pollution. https://doi.org/10.1016/j.scitotenv.2004.04.070

André, M., Hickman, A.J., Hassel, D., Joumard, R., 1995. Driving cycles for emission measurements under European conditions. In: International Congress & Exposition. SAE International. https://doi.org/10.4271/950926

André, M., Joumard, R., Vidon, R., Tassel, P., Perret, P., 2006. Real-world European driving cycles, for measuring pollutant emissions from high- and low-powered cars. Atmos. Environ. 40 (31), 5944–5953. 13th International Symposium on Transport and Air Pollution (TAP-2004). https://doi.org/10.1016/j.atmosenv.2005.12.057

Berzi, L., Delogu, M., Pierini, M., 2016. Development of driving cycles for electric vehicles in the context of the city of florence. Transp. Res. Part D Transport Environ. 47, 299–322. https://doi.org/10.1016/j.trd.2016.05.010

Bhatti, A. H.U., Kazmi, S. A.A., Tariq, A., Ali, G., 2021. Development and analysis of electric vehicle driving cycle for hilly urban areas. Transp. Res. Part D Transport Environ. 99, 103025. https://doi.org/10.1016/j.trd.2021.103025

Bishop, J.D.K., Axon, C.J., 2024. Using natural driving experiments and Markov chains to develop realistic driving cycles. Transp. Res. Part D Transport Environ. 137, 104507. https://doi.org/10.1016/j.trd.2024.104507

Bishop, J. D.K., Axon, C.J., McCulloch, M.D., 2012. A robust, data-driven methodology for real-world driving cycle development. Transp. Res. Part D Transport Environ. 17 (5), 389–397. https://doi.org/10.1016/j.trd.2012.03.003

Brown, S., Bryett, C., Mowle, M., 1999. In-service emissions performance-drive cycles. In: Proposed Diesel Vehicle Emissions National Environmental Protection Measure Preparatory Work. NSW Environment Protection Authority, Motor Vehicle Testing Unit Sydney. Vol. 1.

Cadavid, L., Salazar-Serna, K., 2021. Mapping the research landscape for the motorcycle market policies: sustainability as a trend-a systematic literature review. Sustainability 13 (19). https://doi.org/10.3390/su131910813

Carlson, T.R., Austin, T.C., 1997. Development of Speed Correction Cycles. Technical Report M6.SPD.001. Sierra Research, Inc. Sacramento, California. Prepared for the U.S. Environmental Protection Agency, Contract No. 68-C4-0056, Work Assignment No. 2-01.

Chen, K.S., Wang, W.C., Chen, H.M., Lin, C.F., Hsu, H.C., Kao, J.H., Hu, M.T., 2003. Motorcycle emissions and fuel consumption in urban and rural driving conditions. Sci. Total Environ. 312 (1), 113–122. https://doi.org/10.1016/S0048-9697(03)00196-7

Cossalter, V., 2006. Chapter 3 in *Motorcycle Dynamics*. Lulu Press.

Cox, B.L., Mutel, C.L., 2018. The environmental and cost performance of current and future motorcycles. Appl. Energy 212, 1013–1024. https://doi.org/10.1016/j.apenergy.2017.12.100

Cui, Y., Xu, H., Zou, F., Chen, Z., Gong, K., 2021. Optimization based method to develop representative driving cycle for real-world fuel consumption estimation. Energy 235, 121434. https://doi.org/10.1016/j.energy.2021.121434

Cui, Y., Zou, F., Xu, H., Chen, Z., Gong, K., 2022. A novel optimization-based method to develop representative driving cycle in various driving conditions. Energy 247, 123455. https://doi.org/10.1016/j.energy.2022.123455

Dai, Z., Niemeier, D., Eisinger, D., 2008. Driving cycles: a new cycle-building method that better represents real-world emissions . *Department of Civil and Environmental Engineering, University of California, Davis*, 570, 67.

Dornoff, J., Tietge, U., Mock, P., 2020. On the way to "real-world" CO2 values: the European passenger car market in its first year after introducing the WLTP .

Eccarius, T., and, C.-C.L., 2020. Powered two-wheelers for sustainable mobility: a review of consumer adoption of electric motorcycles. Int. J. Sustainable Transp. 14 (3), 215–231. https://doi.org/10.1080/15568318.2018.1540735

Edwards, A.J., 2022. Aggressive-dynamics metrics for drive-cycle characterization. Transp. Res. Interdiscip. Perspect. 14, 100592. https://doi.org/10.1016/j.trip.2022.100592

Ericsson, E., 1999. The relation between vehicular fuel consumption and exhaust emission and the characteristics of driving patterns. WIT Trans. Built Environ. 44. 11.

Ericsson, E., 2001. Independent driving pattern factors and their influence on fuel-use and exhaust emission factors. Transp. Res. Part D Transport Environ. 6 (5), 325–345. https://doi.org/10.1016/S1361-9209(01)00003-7

Esser, A., Zeller, M., Foulard, S., Rinderknecht, S., 2018. Stochastic synthesis of representative and multidimensional driving cycles. SAE Int. J. Altern. Powertrains 7 (3), 263–272. https://www.jstor.org/stable/26789705.

Gavimath, V.V., Ravuri, S., 2025. Developing real-world drive cycles for heavy-duty freight vehicles using on-board diagnostics data. Transp. Res. Procedia 82, 158–174. World Conference on Transport Research - WCTR 2023 Montreal 17–21 July 2023. https://doi.org/10.1016/j.trpro.2024.12.035

Ghaffarpasand, O., Talaie, M.R., Ahmadikia, H., Khozani, A.T., Shalamzari, M.D., Majidi, S., 2021. Real-world evaluation of driving behaviour and emission performance of motorcycle transportation in developing countries: a case study of isfahan, iran. Urban Clim. 39, 100923. https://doi.org/10.1016/j.uclim.2021.100923

Giakoumis, E.G., 2017. Driving and Engine Cycles. Springer.

Grano, E., Villani, M., de Carvalho Pinheiro, H., Carello, M., 2025. Are we testing vehicles the right way? Challenges of electrified and connected vehicles for standard drive cycles and on-road testing. World Electr. Veh. J. 16 (2). https://doi.org/10.3390/wevj16020094

Gurusamy, A., Ashok, B., 2024. Establishment of electric two-wheeler driving cycle for energy economy and life cycle assessment under indian tier-2 city driving environments. Sustainable Energy Technol. Assess. 66, 103826. https://doi.org/10.1016/j.seta.2024.103826

Guzzella, L., Sciarretta, A., 2007. Vehicle Propulsion System: Introduction to Modeling and Optimization. Springer.

Han, D.S., Choi, N.W., Cho, S.L., Yang, J.S., Kim, K.S., Yoo, W.S., Jeon, C.H., 2012. Characterization of driving patterns and development of a driving cycle in a military area. Transp. Res. Part D: Transport Environ. 17 (7), 519–524. https://doi.org/10.1016/j.trd.2012.06.004

Hull, C., Collett, K.A., McCulloch, M.D., 2024. Developing a representative driving cycle for paratransit that reflects measured data transients: case study in stellenbosch, south africa. Transp. Res. Part A Policy Pract. 181, 103987. https://doi.org/10.1016/j.tra.2024.103987

Hung, W.T., Tong, H.Y., Lee, C.P., Ha, K., Pao, L.Y., 2007. Development of a practical driving cycle construction methodology: a case study in Hong Kong. Transp. Res. Part D: Transport Environ. 12 (2), 115–128. https://doi.org/10.1016/j.trd.2007.01.002

IEA, 2024. Trends in Other Light-Duty Electric Vehicles. IEA. https://www.iea.org/reports/global-ev-outlook-2024.

IPCC, 2022. Climate Change 2022: Impacts, Adaptation, and Vulnerability. Cambridge University Press, Cambridge, UK and New York, NY, USA. chapter IPCC, 2022: Summary for Policymakers. pp. 3–33.

Lot, R., Sadauckas, J., 2021. Motorcycle Design: Vehicle Dynamics Concepts and Applications.

Jia, X., Wang, H., Xu, L., Wang, Q., Li, H., Hu, Z., Li, J., Ouyang, M., 2021. Constructing representative driving cycle for heavy duty vehicle based on markov chain method considering road slope. Energy AI 6, 100115. https://doi.org/10.1016/j.egyai.2021.100115

Gao, Y., Chen, L., Ehsani, M., 1999. Investigation of the Effectiveness of Regenerative Braking for EV and HEV. *SAE Transactions*, 108, 3184–3190. SAE International. http://www.jstor.org/stable/44733986.

Koossalapeerom, T., Satiennam, T., Satiennam, W., Leelapatra, W., Seedam, A., Rakpukdee, T., 2019. Comparative study of real-world driving cycles, energy consumption, and CO2 emissions of electric and gasoline motorcycles driving in a congested urban corridor. Sustainable Cities Soc. 45, 619–627. https://doi.org/10.1016/j.scs.2018.12.031

Kruse, R.E., Huls, T.A., 1973. Development of the federal urban driving schedule . *SAE Technical Paper 730553*. SAE International. https://doi.org/10.4271/730553.

Kumar, R., Durai, B.K., Saleh, W., Boswell, C., 2011. Comparison and evaluation of emissions for different driving cycles of motorcycles: a note. Transp. Res. Part D Transport Environ. 16 (1), 61–64. https://doi.org/10.1016/j.trd.2010.08.006

Kusalaphirom, T., Satiennam, T., Satiennam, W., Seedam, A., 2022. Development of a real-world eco-driving cycle for motorcycles. Sustainability 14 (10). https://doi.org/10.3390/su14106176

Lee, G., Yeon, J., Kim, N., Park, S., 2025. A comprehensive methodology for developing and evaluating driving cycles for electric vehicles using real-world data. eTransportation 24, 100409. https://doi.org/10.1016/j.etran.2025.100409

Lee, T.-K., Filipi, Z., 2011. Synthesis of real-world driving cycles using stochastic process and statistical methodology. Int. J. Veh. Des. 57, 17–36. https://doi.org/10.1504/IJVD.2011.043590

Lien, N., Duc, K., Le Anh, T., 2024. Estimating the Difference Between Actual Driving Characteristics and World Motorcycle Test Cycle: A Case Study for Motorcycles in Hanoi. pp. 492–503. https://doi.org/10.1007/978-3-031-62238-0_51

Lin, J., Niemeier, D.A., 2002. An exploratory analysis comparing a stochastic driving cycle to california's regulatory cycle. Atmos. Environ. 36 (38), 5759–5770. https://doi.org/10.1016/S1352-2310(02)00695-7

Lin, J., Niemeier, D.A., 2003. Regional driving characteristics, regional driving cycles. Transp. Res. Part D Transport Environ. 8 (5), 361–381. https://doi.org/10.1016/S1361-9209(03)00022-1

Ma, R., He, X., Zheng, Y., Zhou, B., Lu, S., Wu, Y., 2019. Real-world driving cycles and energy consumption informed by large-sized vehicle trajectory data. J. Clean Prod. 223, 564–574. https://doi.org/10.1016/j.jclepro.2019.03.002

Maharaj, B.S., King, G., 2023. Representative driving cycles for trinidad and tobago with slope profiles for electric vehicles. Transp. Res. Rec. 2677 (5), 1007–1016. https://doi.org/10.1177/03611981221138526

Mahmoud M. Kamel, Muhammed A. Hassan, H.S., Huzayyin, O.A., 2024. Comparative studies of Markov chain-based driving cycles for light-duty vehicles. Transp. Plann. Technol. 47 (5), 749–787. https://doi.org/10.1080/03081060.2023.2294343

United Nations Economic Commission for Europe (UNECE), 2014. Economic Commission for Europe, Inland Transport Committee: World Forum for Harmonization of Vehicle Regulations. Executive Committee (AC.3) of the 1998 Global Agreement. ECE/TRANS/WP.29/AC.3/26. Technical Report.

Nyberg, P., Frisk, E., Nielsen, L., 2014. Generation of equivalent driving cycles using markov chains and mean tractive force components. IFAC Proc. Volumes 47 (3), 8787–8792. 19th IFAC World Congress. https://doi.org/10.3182/20140824-6-ZA-1003.02239

O'Keefe, M., Simpson, A., Kelly, K., Pedersen, D., 2007. Duty cycle characterization and evaluation towards heavy hybrid vehicle applications. Warrendale PA Soc. Automot. Eng. . https://doi.org/10.4271/2007-01-0302

Park, J., Seo, J., Park, S., 2023. Development of vehicle emission rates based on vehicle-specific power and velocity. Sci. Total Environ. 857, 159622. https://doi.org/10.1016/j.scitotenv.2022.159622

Peng, Y., Zhuang, Y., Yang, Y., 2020. A driving cycle construction methodology combining K-means clustering and Markov model for urban mixed roads. Proc. Inst. Mech. Eng. Part D J. Automob. Eng. 234 (2–3), 714–724. https://doi.org/10.1177/0954407019848873

Qiu, H., Cui, S., Wang, S., Wang, Y., Feng, M., 2022. A clustering-based optimization method for the driving cycle construction: a case study in fuzhou and putian, china. IEEE Trans. Intell. Transp. Syst. 23 (10), 18681–18694. https://doi.org/10.1109/TITS.2022.3160275

Quirama, L.F., Giraldo, M., Huertas, J.I., Tibaquirá, J.E., Cordero-Moreno, D., 2021. Main characteristic parameters to describe driving patterns and construct driving cycles. Transp. Res. Part D Transp. Environ. 97, 102959. https://doi.org/10.1016/j.trd.2021.102959

Saleh, W., Kumar, R., Kirby, H., Kumar, P., 2009. Real world driving cycle for motorcycles in edinburgh. Transp. Res. Part D Transport Environ. 14 (5), 326–333. https://doi.org/10.1016/j.trd.2009.03.003

Salihu, F., Demir, Y.K., Demir, H.G., 2023. Effect of road slope on driving cycle parameters of urban roads. Transp. Res. Part D Transport Environ. 118, 103676. https://doi.org/10.1016/j.trd.2023.103676

Seedam, A., Satiennam, T., Radpukdee, T., Satiennam, W., 2015. Development of an onboard system to measure the on-road driving pattern for developing motorcycle driving cycle in khon kaen city, thailand. IATSS Res. 39 (1), 79–85. https://doi.org/10.1016/j.iatssr.2015.05.003

Shi, S., Lin, N., Zhang, Y., Cheng, J., Huang, C., Liu, L., Lu, B., 2016. Research on Markov property analysis of driving cycles and its application. Transp. Res. Part D Transport Environ. 47, 171–181. https://doi.org/10.1016/j.trd.2016.05.013

Silvas, E., Hereijgers, K., Peng, H., Hofman, T., Steinbuch, M., 2016. Synthesis of realistic driving cycles with high accuracy and computational speed, including slope information. IEEE Trans. Veh. Technol. 65 (6), 4118–4128. https://doi.org/10.1109/TVT.2016.2546338

Sithananthan, M., Kumar, R., 2021. A framework for development of real-world motorcycle driving cycle in india. Proc. Inst. Mech. Eng. Part D J. Automob. Eng. 235 (6), 1497–1515. https://doi.org/10.1177/0954407020977533

Tong, H.Y., 2019. Development of a driving cycle for a supercapacitor electric bus route in Hong Kong. Sustainable Cities Soc. 48, 101588. https://doi.org/10.1016/j.scs.2019.101588

Tong, H.Y., Hung, W.T., Cheung, C.S., 1999. Development of a driving cycle for hong kong. Atmos. Environ. 33 (15), 2323–2335. https://doi.org/10.1016/S1352-2310(99)00074-6

Tong, H.Y., Ng, K.W., 2023. Developing electric bus driving cycles with significant road gradient changes: a case study in Hong Kong. Sustainable Cities Soc. 98, 104819. https://doi.org/10.1016/j.scs.2023.104819

Tong, H.Y., Tung, H.D., Hung, W.T., Nguyen, H.V., 2011. Development of driving cycles for motorcycles and light-duty vehicles in vietnam. Atmos. Environ. 45 (29), 5191–5199. https://doi.org/10.1016/j.atmosenv.2011.06.023

Topić, J., Škugor, B., Deur, J., 2020. Analysis of Markov chain-based methods for synthesis of driving cycles of different dimensionality. In: 2020IEEE 23rd International Conference on Intelligent Transportation Systems (ITSC), pp. 1–8. https://doi.org/10.1109/ITSC45102.2020.9294302

Topić, J., Škugor, B., Deur, J., 2021. Synthesis and feature selection-supported validation of multidimensional driving cycles. Sustainability 13 (9). https://doi.org/10.3390/su13094704

Tran, D.-S., Le, H., Posada, F., 2023. Total cost of ownership comparison for electric two-wheelers in vietnam . The International Council on Clean Transportation (ICCT). Technical Report. 19.

Truong, N., Trencher, G., Yarime, M., Barrett, B., Matsubae, K., 2024. Barriers to the adoption of electric cars and electric motorcycles in vietnam. Transp. Res. Part D Transport Environ. 131, 104204. https://doi.org/10.1016/j.trd.2024.104204

Tsai, J.-H., Chiang, H.-L., Hsu, Y.-C., Peng, B.-J., Hung, R.-F., 2005. Development of a local real world driving cycle for motorcycles for emission factor measurements. Atmos. Environ. 39 (35), 6631–6641. https://doi.org/10.1016/j.atmosenv.2005.07.040

Tzeng, G.-H., Chen, J.-J., 1998. Developing a Taipei motorcycle driving cycle for emissions and fuel economy. Transp. Res. Part D Transport Environ. 3 (1), 19–27. https://doi.org/10.1016/S1361-9209(97)00008-4

Wang, X., Li, T., Chen, X., Li, B., 2020. Construction of driving cycle: a study based on PCA, k-means, and GA. In: 2020 7th International Conference on Information Science and Control Engineering (ICISCE), pp. 1785–1789. https://doi.org/10.1109/ICISCE50968.2020.00351

Wang, Z., Zhang, J., Liu, P., Qu, C., Li, X., 2019. Driving cycle construction for electric vehicles based on Markov chain and Monte Carlo method: a case study in Beijing. Energy Procedia 158, 2494–2499. Innovative Solutions for Energy Transitions. https://doi.org/10.1016/j.egypro.2019.01.389

Weiss, M., Dekker, P., Moro, A., Scholz, H., Patel, M.K., 2015. On the electrification of road transportation - a review of the environmental, economic, and social performance of electric two-wheelers. Transp. Res. Part D Transport Environ. 41, 348–366. https://doi.org/10.1016/j.trd.2015.09.007

Xiao, Z., Dui-Jia, Z., Jun-Min, S., 2012. A synthesis of methodologies and practices for developing driving cycles. Energy Procedia 16, 1868–1873. 2012 International Conference on Future Energy, Environment, and Materials. https://doi.org/10.1016/j.egypro.2012.01.286

Yang, D.P., Liu, T., Zhang, X.M., Zeng, X.H., Song, D.F., 2023. Construction of high-precision driving cycle based on metropolis-hastings sampling and genetic algorithm. Transp. Res. Part D Transport Environ. 118, 103715. https://doi.org/10.1016/j.trd.2023.103715

Ye, Y., Zhao, X., Zhang, J., 2023. Driving cycle electrification and comparison. Transp. Res. Part D Transport Environ. 123, 103900. https://doi.org/10.1016/j.trd.2023.103900

Yuniaristanto, Y., Utami, M.W.D., Sutopo, W., Hisjam, M., 2022. Investigating key factors influencing purchase intention of electric motorcycle in indonesia. Trans. Transport Sci. 13 (1), 54–64.